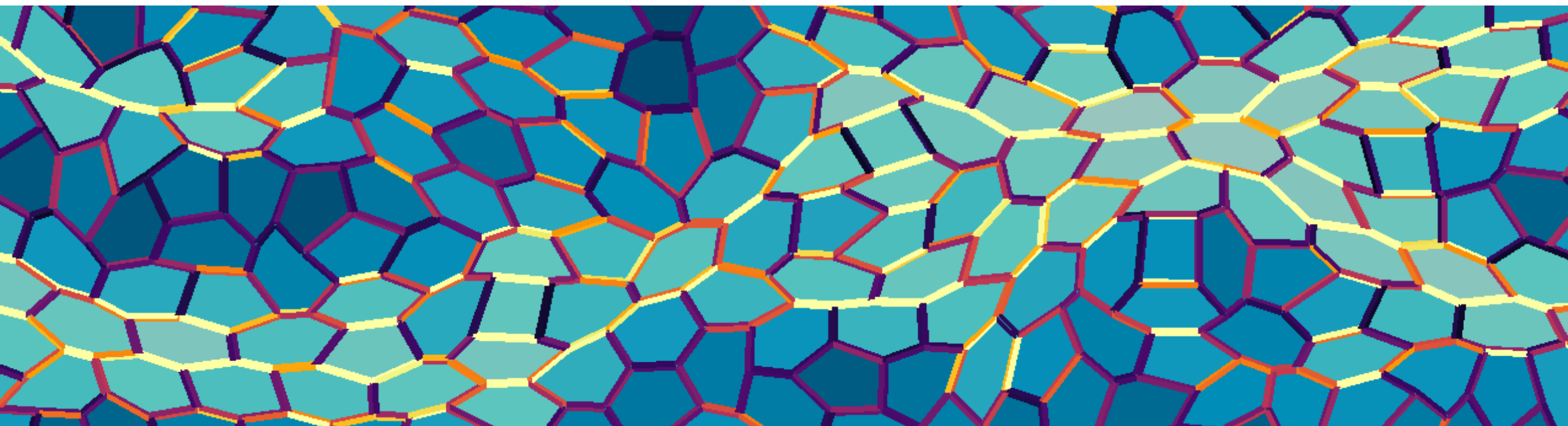


Building microscopic models of cell sheets

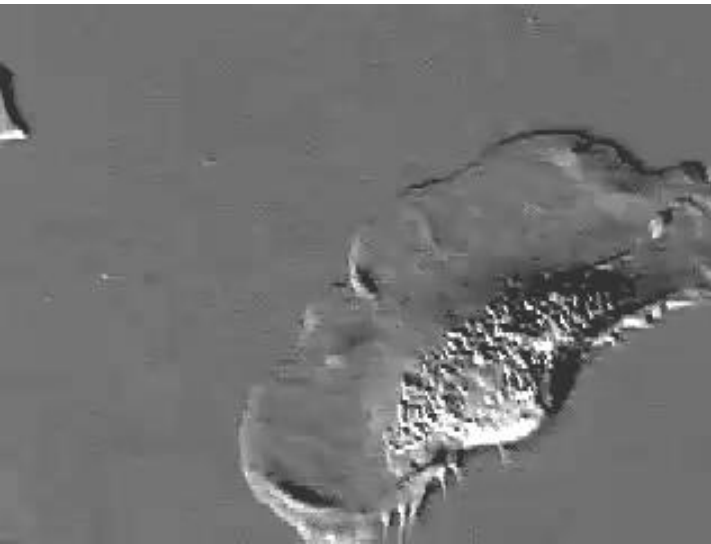


Silke Henkes, Lorentz Institute, Leiden University, The Netherlands

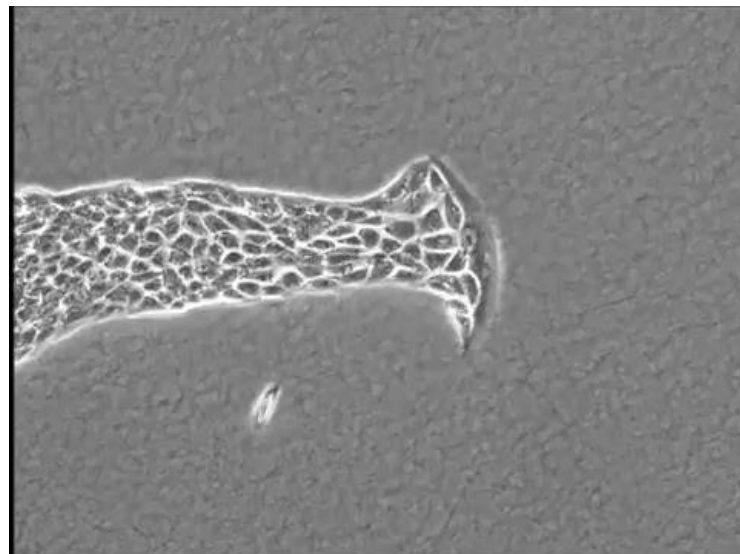
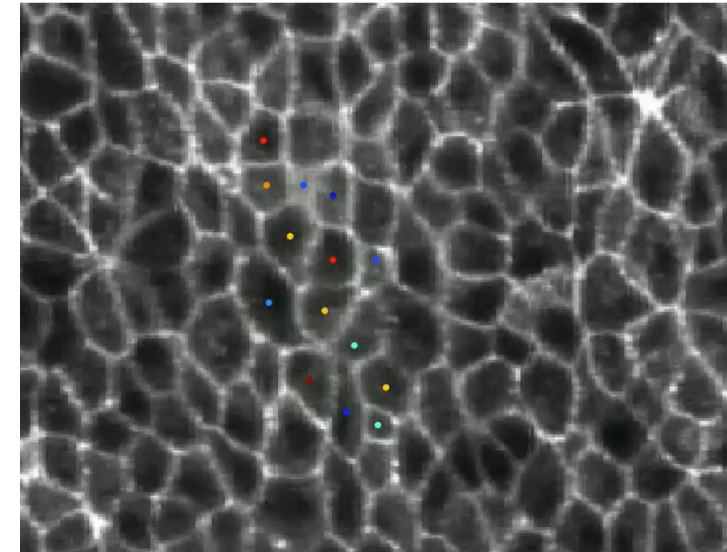


Collective motion of cells

Fibroblast cell crawling

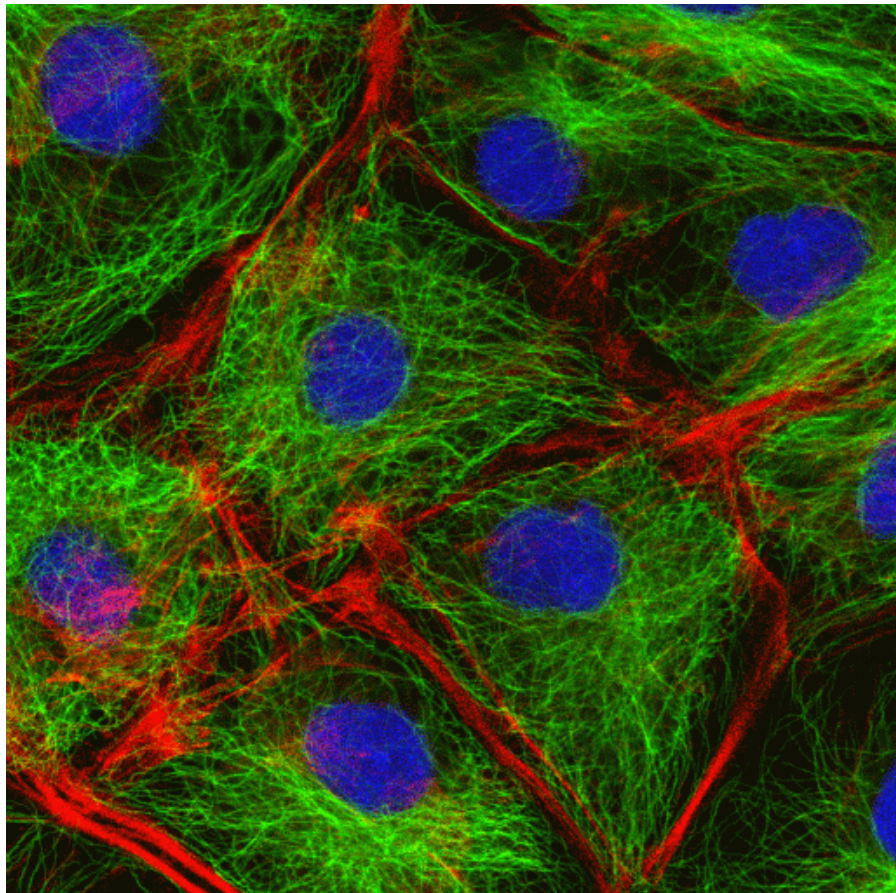


Chick embryo development

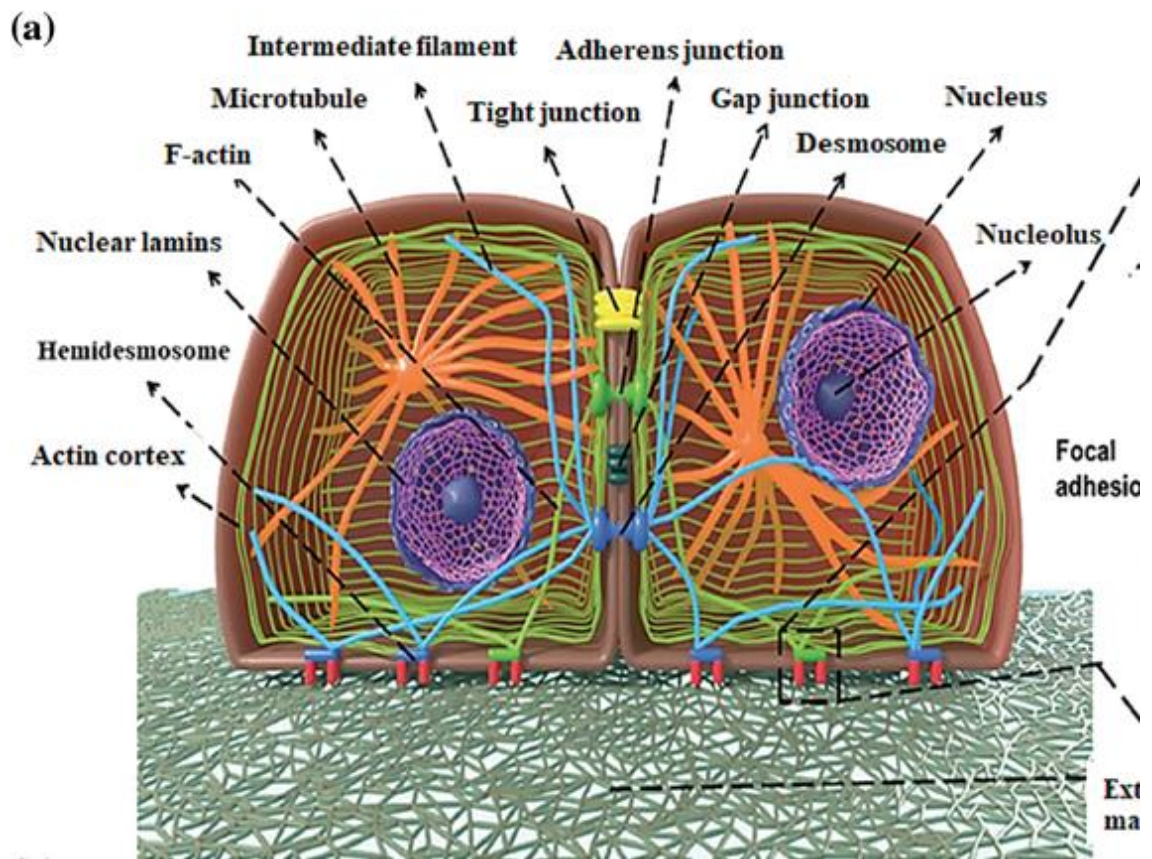


Epithelial cells on
a substrate
moving into a new
area

The ingredients of a cell



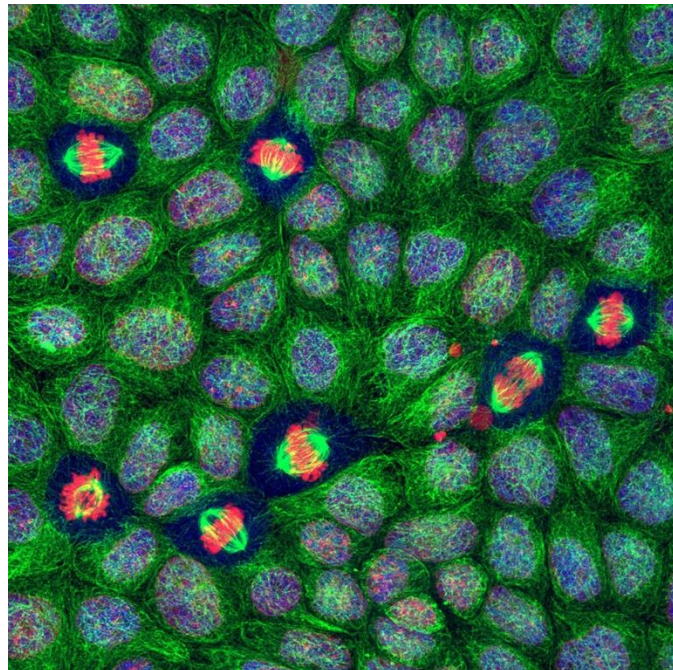
British society for cell biology



D. Septiadi et al., 2018

Epithelial cell sheets

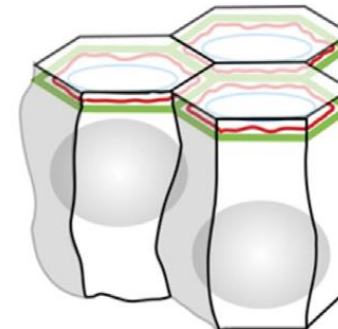
Cells in a MDCK monolayer (top view)



Green: Actin cytoskeleton

Blue: Cell nucleus

Red: histones (cell division)



Side view: like a
cobblestone
pavement

Epithelia in real organisms: a variety
of shapes, and also layered

Types of Epithelium



Simple squamous

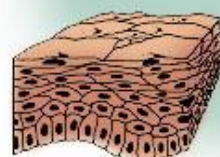


Simple cuboidal

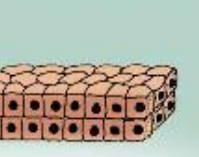


Simple columnar

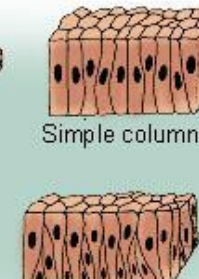
Transitional



Stratified squamous



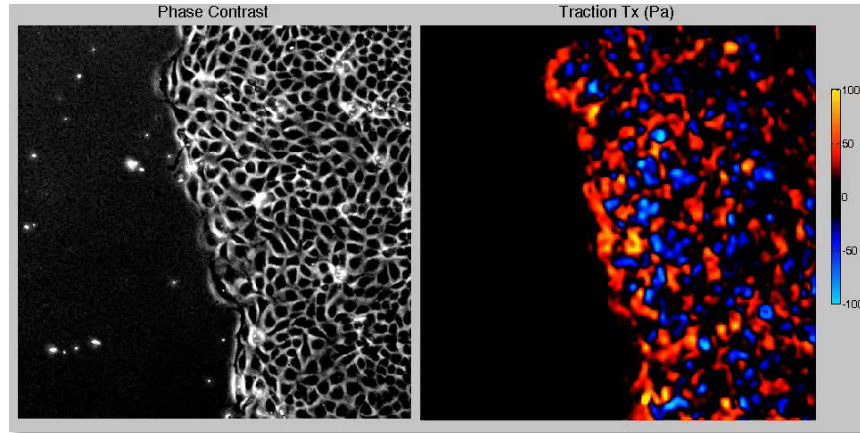
Stratified cuboidal



Pseudostratified columnar

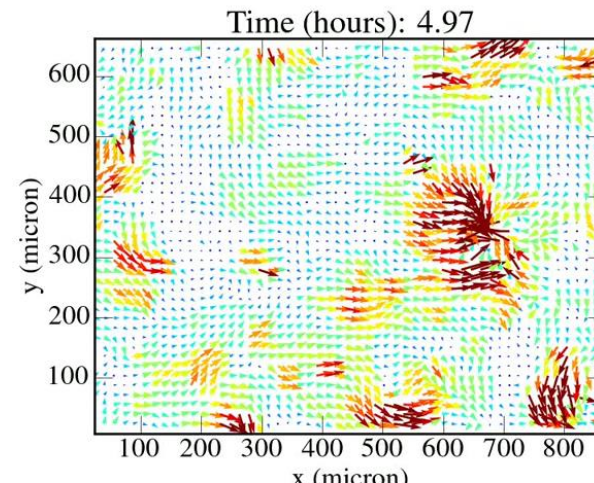
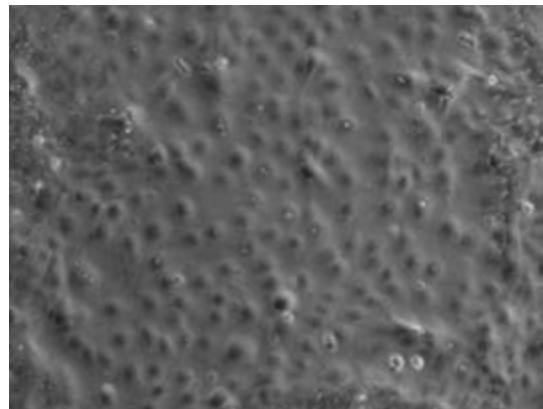
Collective cell mechanics in epithelial cell sheets

‘Swirly’ correlated motion patterns



X. Trepat et al.,
Nature Phys. 2009,
T. Angelini et al.,
PNAS 2011

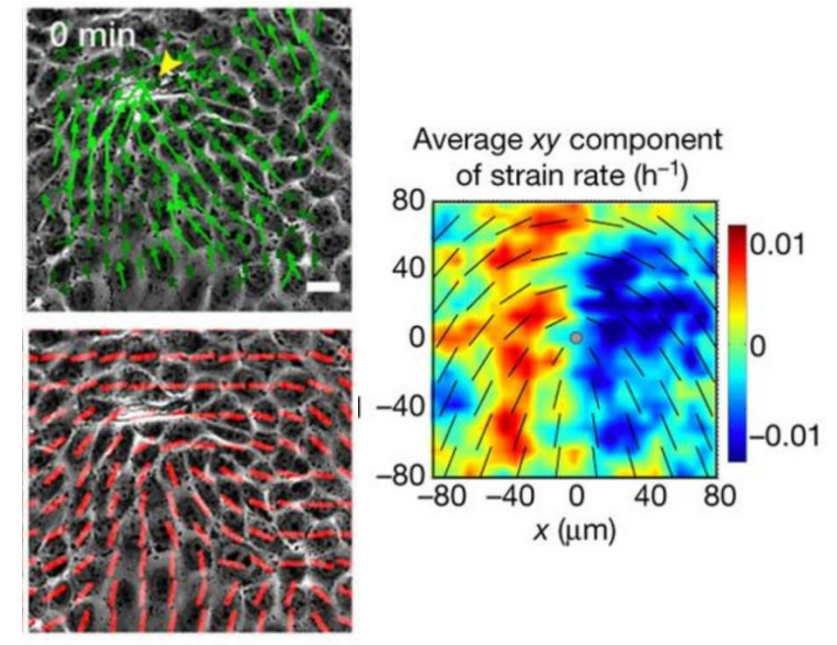
Generic feature, e.g: Human corneal epithelial cell sheet



Kaja Kostanjevec

Active nematic properties with topological defects

Moving +1/2 defects, T. B. Saw et al, Nature 544, 212 (2017), Balasumbramanian et al (2021)

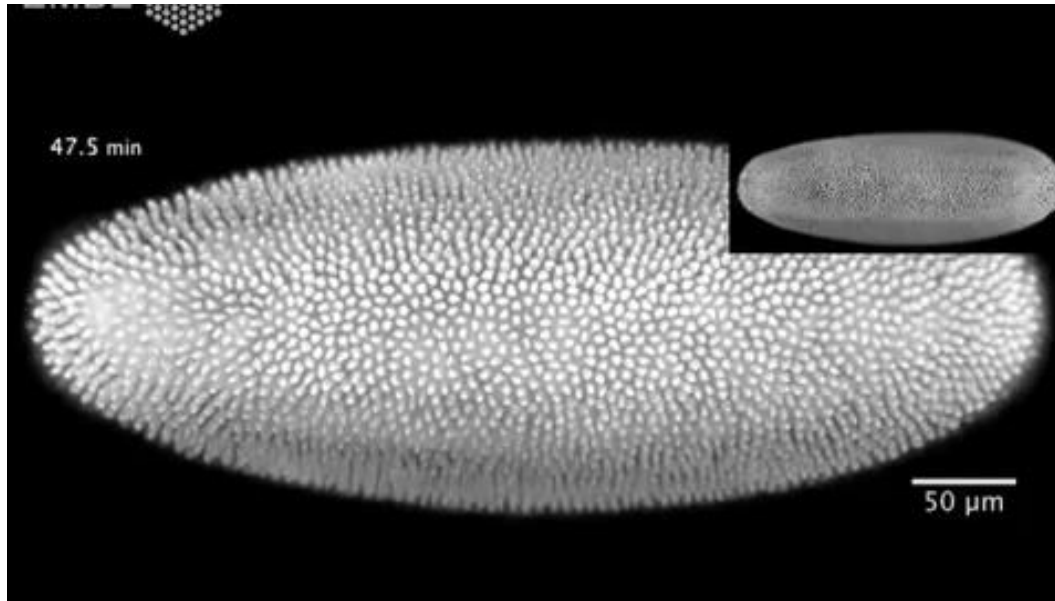


Collective cell mechanics in development

Fruit fly (*drosophila*) gastrulation

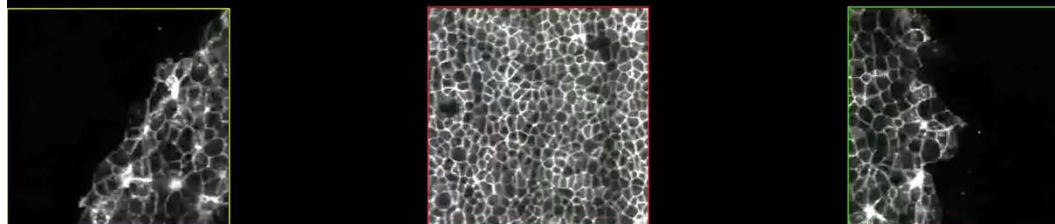
First step in the development of the embryo

European Molecular Biology Laboratory (EMBL)

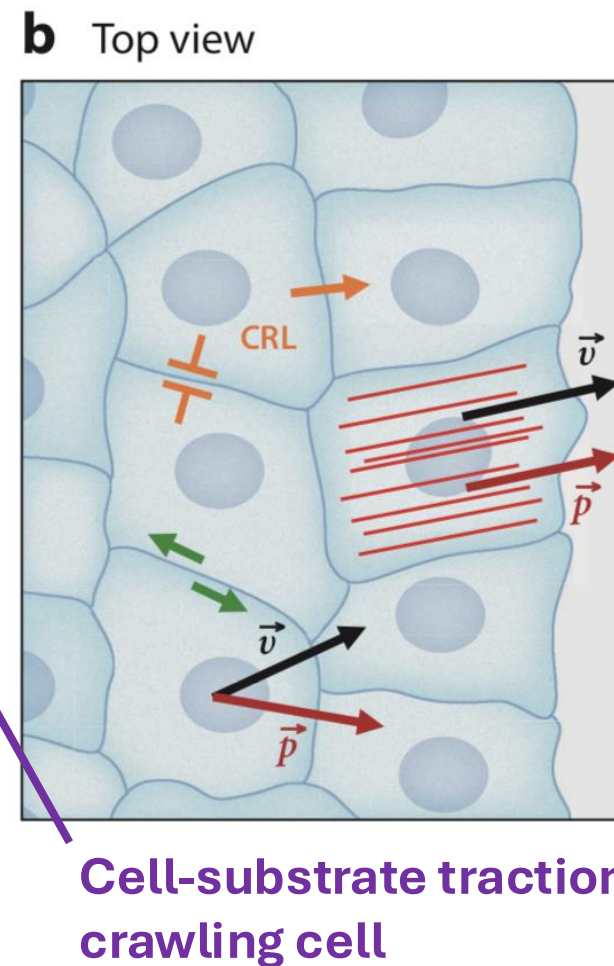
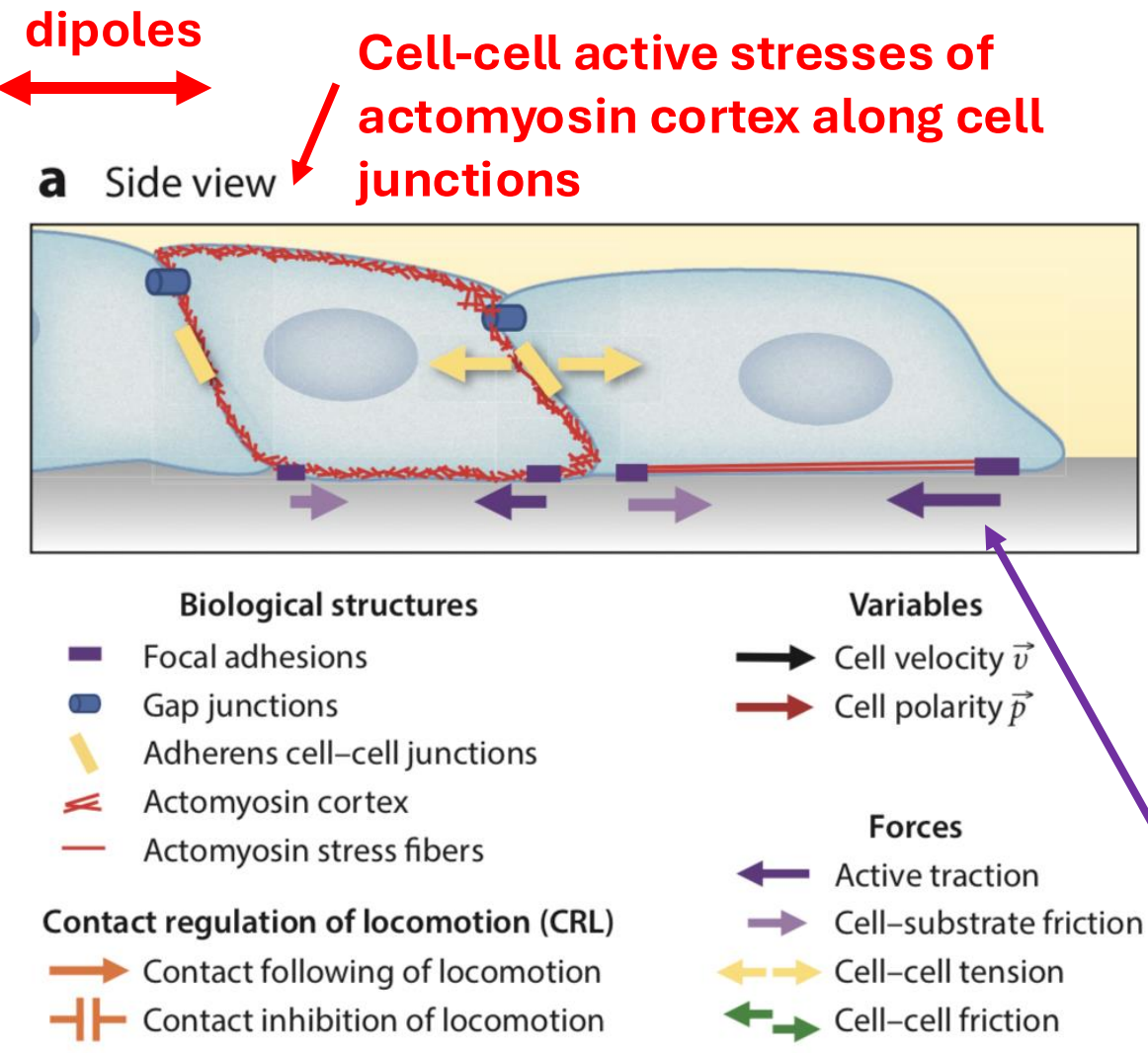


Primitive streak formation (gastrulation in the chick embryo)

E. Rozbicki et al, Nature Cell Biology 17, 397–408 (2015)

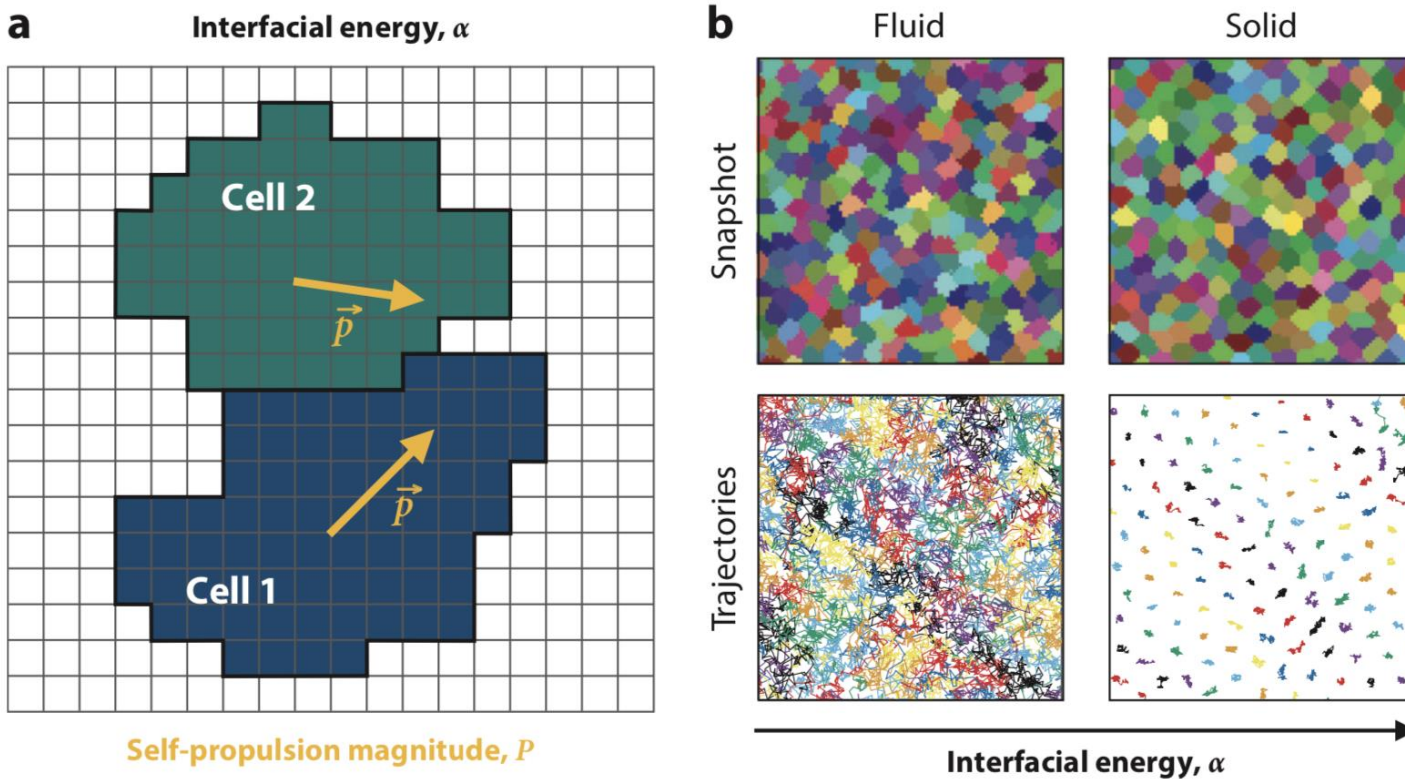


Mechanisms of activity



R. Alert and X. Trepat,
Ann. Rev. Cond. Mat.
Phys. 2020

Other approaches: Cellular Potts models



Minimise effective Hamiltonian, Monte Carlo approach, not true dynamics
(in its simplest forms)

$$\mathcal{H} = \sum_{\langle i,j \rangle} J(\sigma_i, \sigma_j) + \lambda \sum_{\sigma=1}^{m-1} (A_\sigma - A_0)^2 - P \sum_{\sigma=1}^{m-1} \vec{R}_\sigma \cdot \vec{p}_\sigma.$$

Interaction (spins)

Area constraint

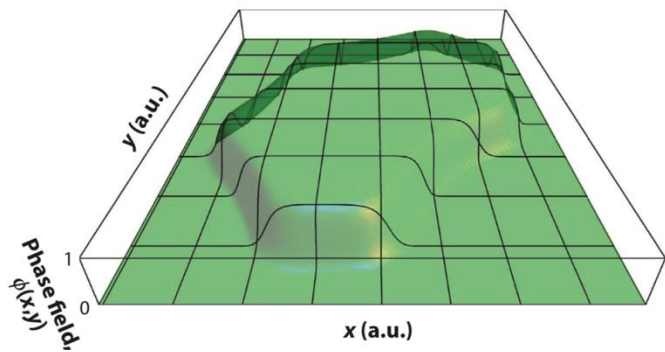
Migration / polarity

Other approaches: Phase field models

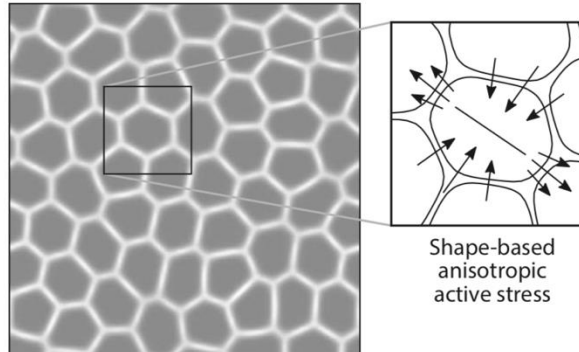
Different scalar field ϕ_i for every cell. Simulate overdamped dynamics of many interacting cells:

$$\partial_t \phi_i + \vec{v}_i \cdot \vec{\nabla} \phi_i = -\frac{\delta \mathcal{F}}{\delta \phi_i}$$

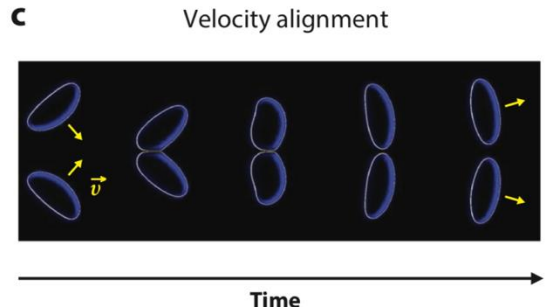
a



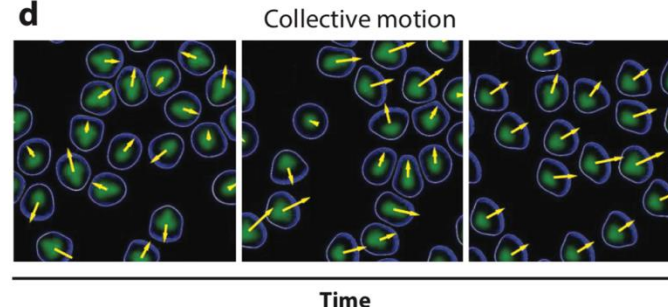
b



c



d



$$\mathcal{F}_{\text{CH}} = \sum_{i=1}^N \frac{\gamma}{\epsilon} \int_{\mathcal{A}} \left[4\phi_i^2(1-\phi_i)^2 + \epsilon^2 |\vec{\nabla} \phi_i|^2 \right] d^2 \vec{r},$$

$$\mathcal{F}_{\text{area}} = \sum_{i=1}^N \mu \left(1 - \frac{1}{\pi R^2} \int_{\mathcal{A}} \phi_i^2 d^2 \vec{r} \right)^2,$$

$$\mathcal{F}_{\text{cell-cell}} = \sum_{i=1}^N \sum_{j \neq i} \frac{\kappa}{\epsilon} \int_{\mathcal{A}} \left[\phi_i^2 \phi_j^2 - \tau \epsilon^4 |\vec{\nabla} \phi_i|^2 |\vec{\nabla} \phi_j|^2 \right] d^2 \vec{r}.$$

Total free energy is sum of Cahn-Hilliard (phase separation), area constraint and cell-cell interaction terms:

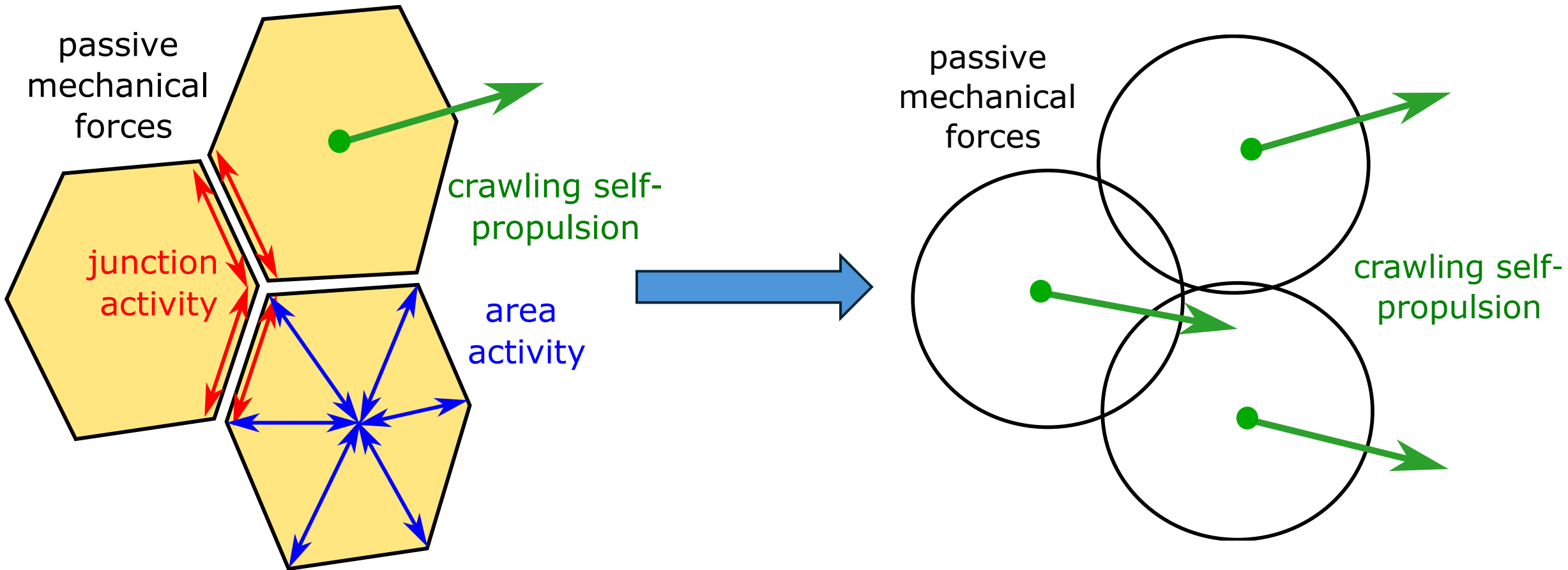
Outline: Making models of tissues

- I. Active Brownian particles: The simplest model – a demonstration
- II. Vertex model with crawling activity: The self-propelled Voronoi (SPV) model
- III. Vertex models with microscopic activity: Forces on junctions, and a zoo of new kinds of activity

Outline: Making models of tissues

- I. **Active Brownian particles: The simplest model – a demonstration**
- II. Vertex model with crawling activity: The self-propelled Voronoi (SPV) model
- III. Vertex models with microscopic activity: Forces on junctions, and a zoo of new kinds of activity

Simplest approximation: Self-propelled round particles



Active matter: Collective motion out of thermal equilibrium



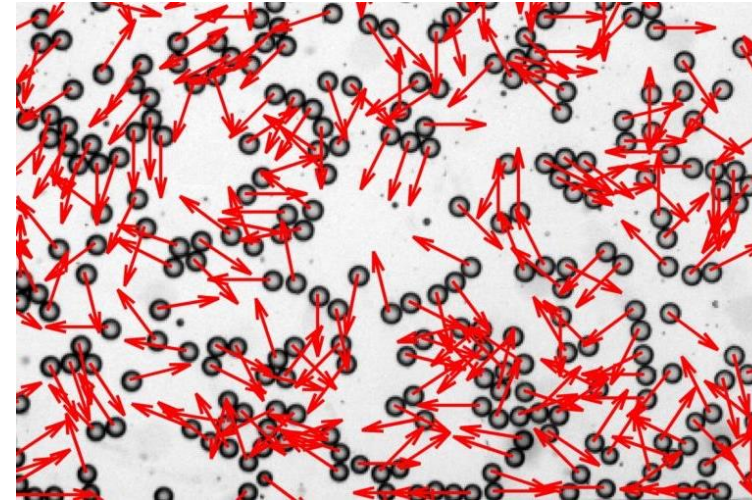
Artificial collective motion

Robot swarms



M. Rubinstein et al., Science 345 (2014)

Active Colloids



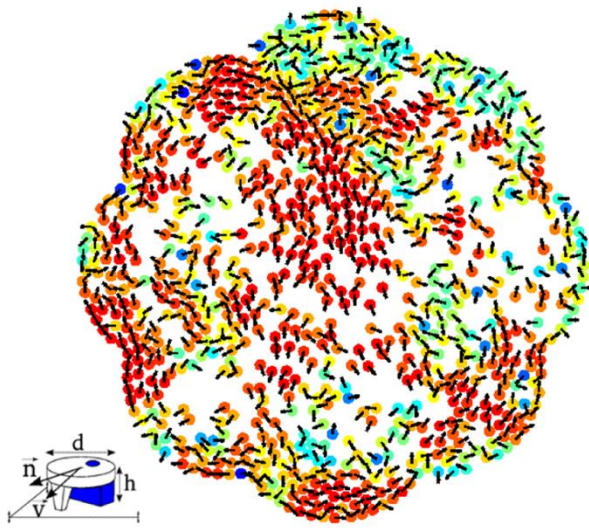
S. Thutupalli et al., NJP 13, 073021

Self-propelled mechanical
disks

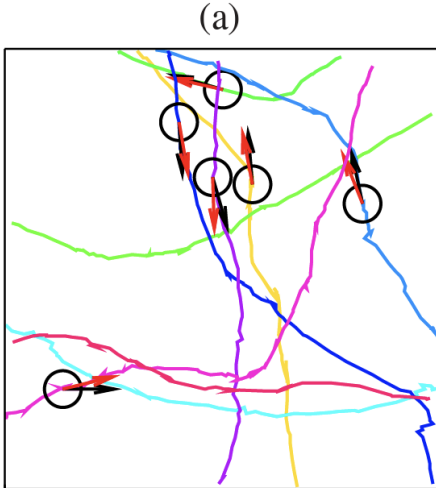


Dauchot lab, ESPCI

Mechanical active particles



J. Deseigne et al, PRL 105,098001 (2010)



- Move by differential friction together with vibration of the substrate (plate) or internal vibration (bristle bots / robots).
- Many different motility models and shapes
- Also perform a persistent random walk



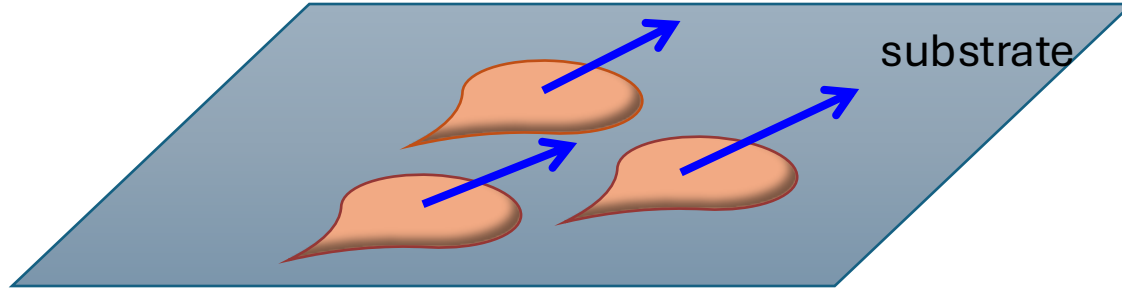
Hexbots (type of bristle bot)



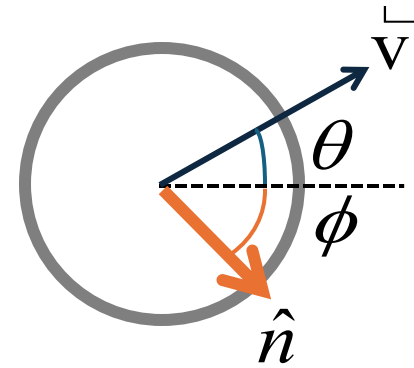
Chalks with rubber providing differential friction tracing trajectories on vibrated plates.

(SH, art project with Daksha Patel, 2019)

Active Brownian particles



- Particles move over a substrate or through a fluid with friction. We work at the micron scale, so mass is negligible: overdamped equations
- Self-propulsion is an internally generated force in a direction \mathbf{n}
- Particles interact with each other through short - ranged repulsion and attraction forces



$$\zeta \dot{\mathbf{r}}_i = F_{\text{act}} \hat{\mathbf{n}}_i + \sum_j \mathbf{F}_{ij} + \eta_i$$

self-propulsion
force j noise
 short-range forces

Overdamped
Langevin equation
with extra active force
term

- Dynamics of \mathbf{n} determines active behaviour: Rotational diffusion

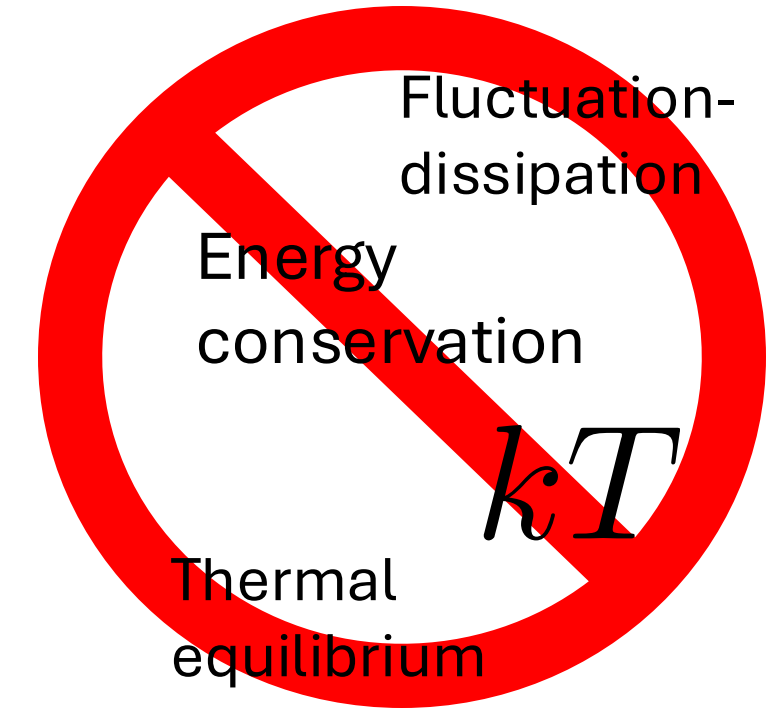
$$\dot{\phi} = \eta, \quad \langle \eta(t) \eta(t') \rangle = \frac{1}{\tau_r} \delta(t - t')$$

$$D_R = 1/\tau_r$$

Physics of active matter: Out of thermal equilibrium

Requires a very nuanced approach:

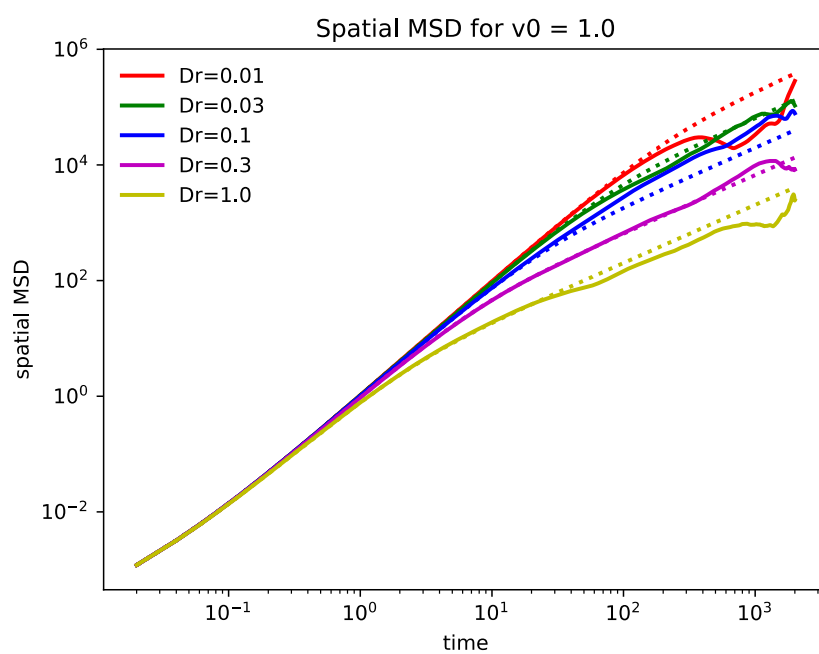
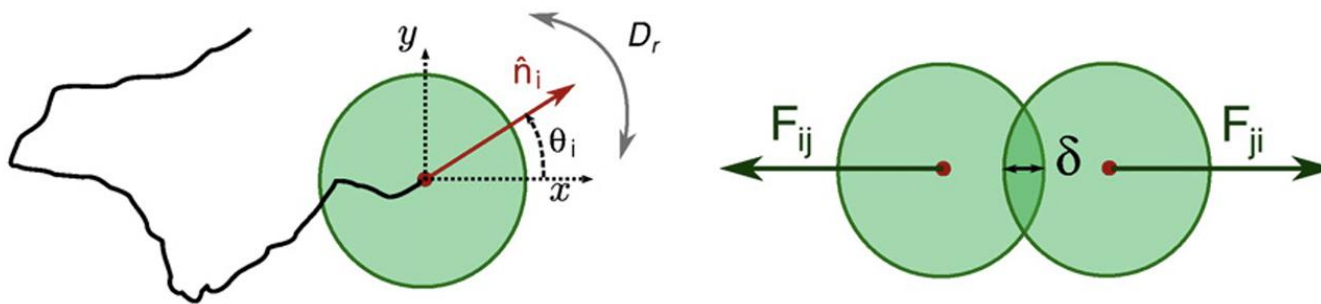
- Carefully adapt equilibrium physics results, e.g. Langevin equations work, but Smoluchowsky don't.
- Effective continuum models based on methods that we developed for continuum mechanics (e.g. active liquid crystals)
- Direct simulations of active systems



Derivation on the board: One active Brownian particle

One active Brownian particle

Performs persistent random walk: See board derivation and active notes on Brightspace

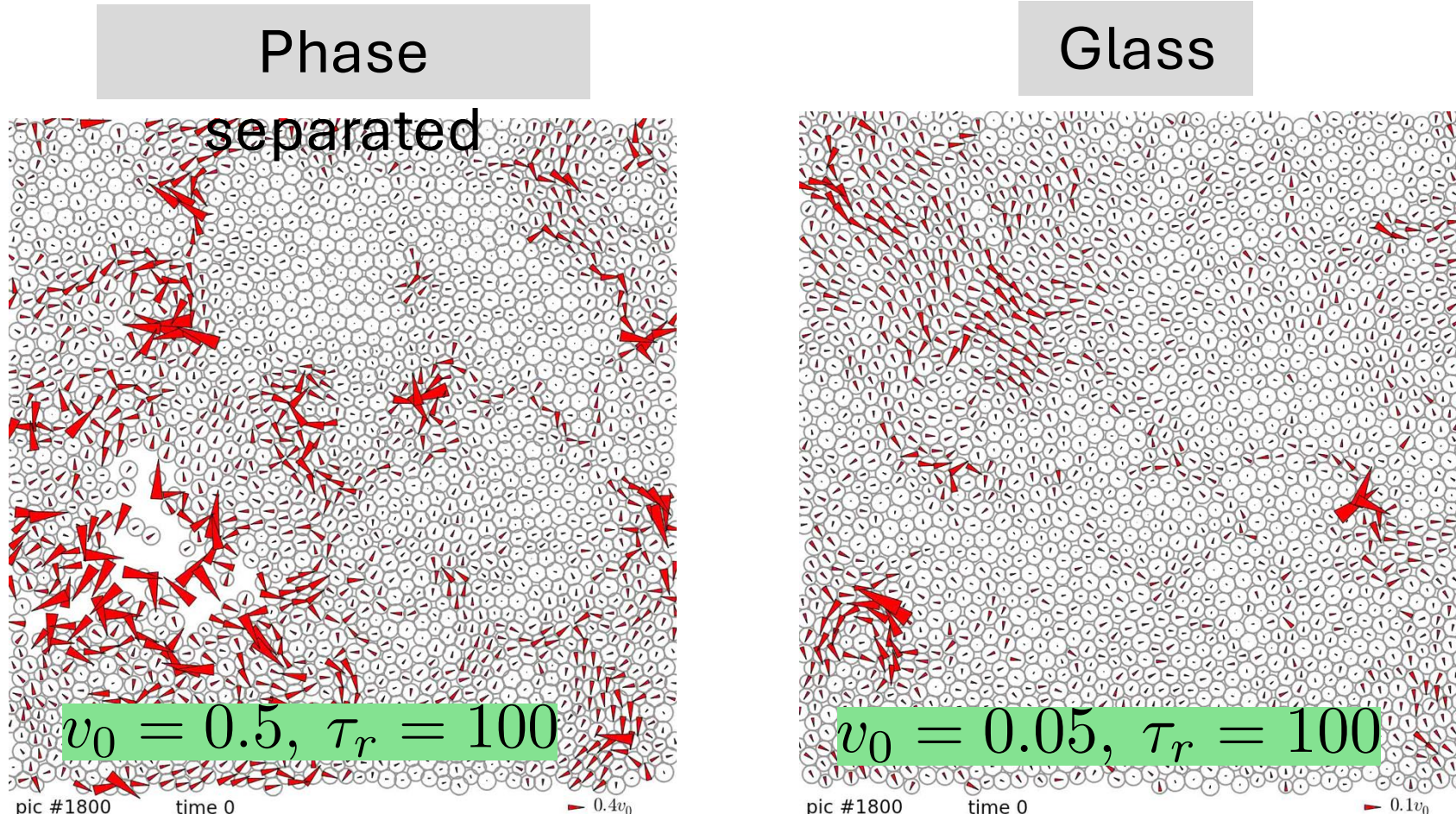


M.C. Marchetti et al, Current
Opinion in Colloid & Interface
Science, 21, 34-43 (2016)

See exercise set 4: Simulate and
analyse motion of a single ABP

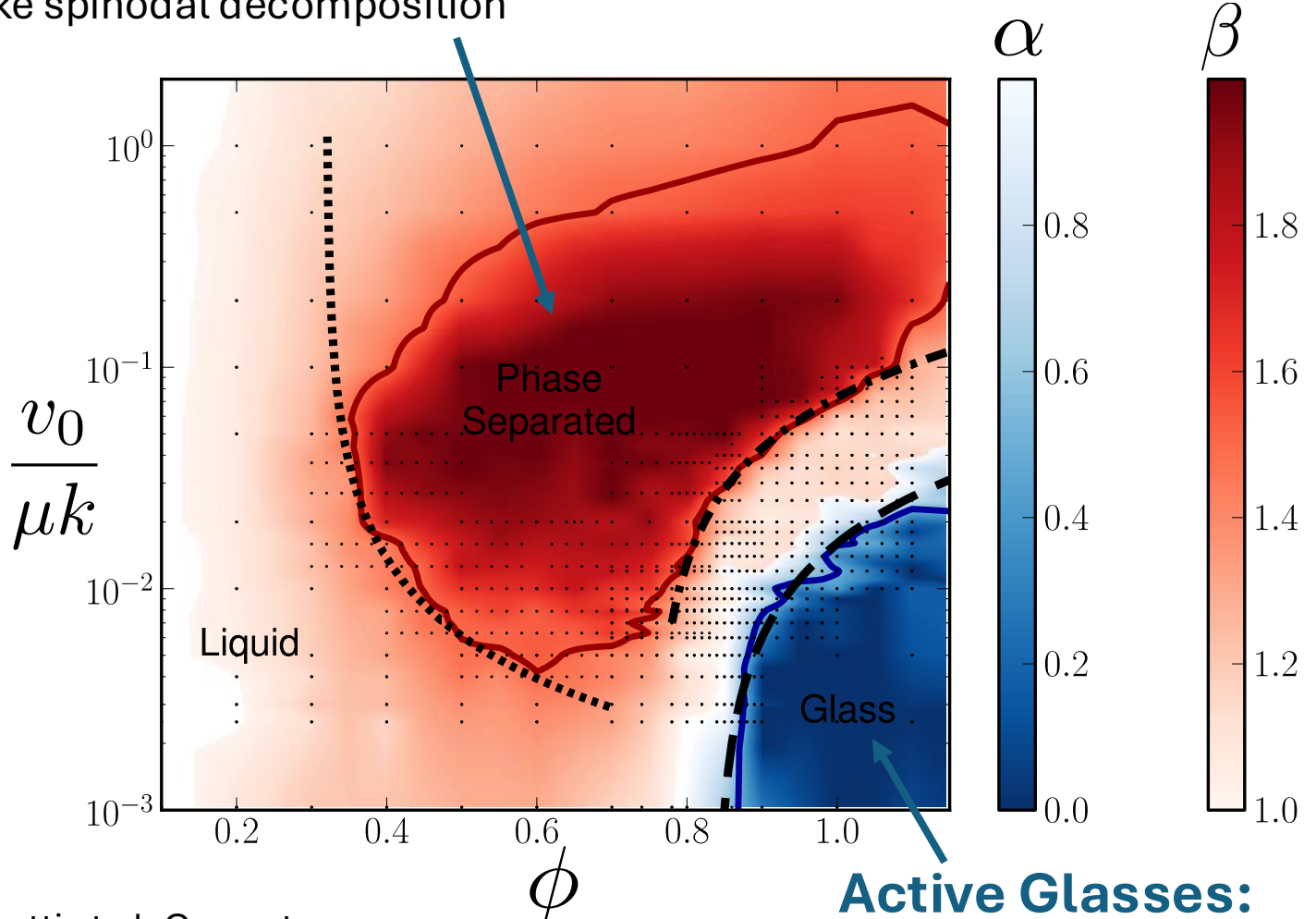
Collective motion of Active Brownian particles

$$\dot{\phi} = \eta, \quad \langle \eta(t)\eta(t') \rangle = \frac{1}{\tau_r} \delta(t - t') \quad \text{Diffusive angular dynamics}$$



Motility-induced phase separation:

Velocity slows down with density due to collisions
Leads to liquid-gas like spinodal decomposition



M.C. Marchetti et al, Current
Opinion in Colloid & Interface
Science, 21, 34-43 (2016)

Active Glasses:

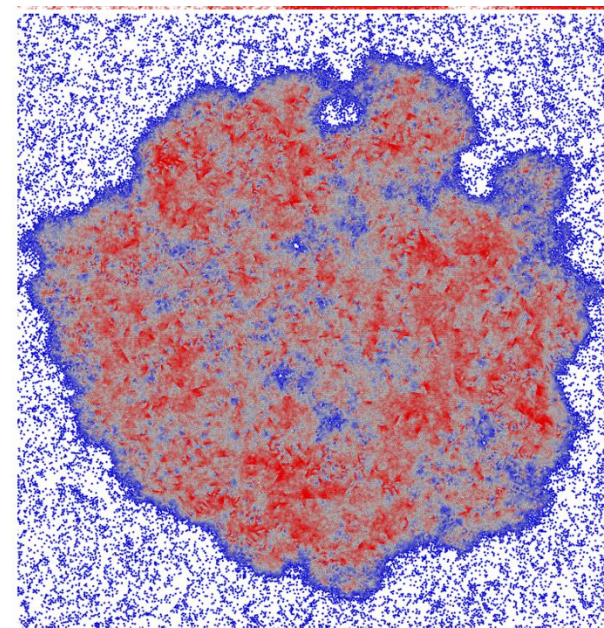
Driving too low to push particles past each other at high density. Shares properties with both thermal glasses and sheared athermal packings

MIPS phase

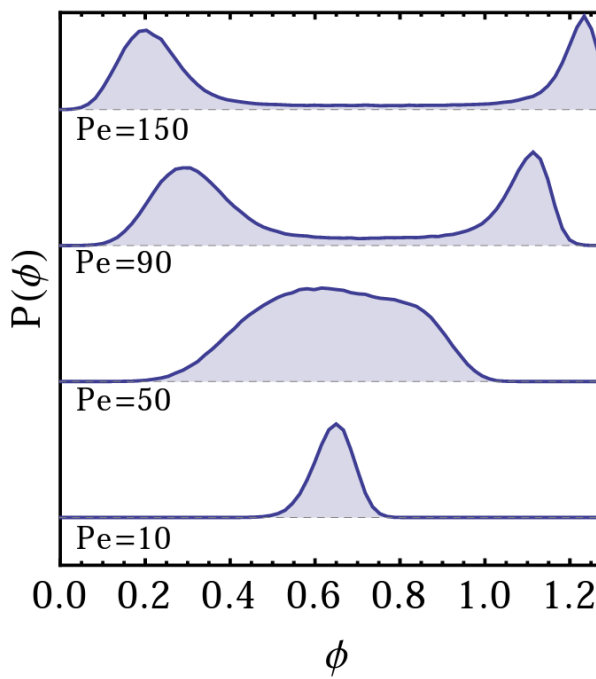
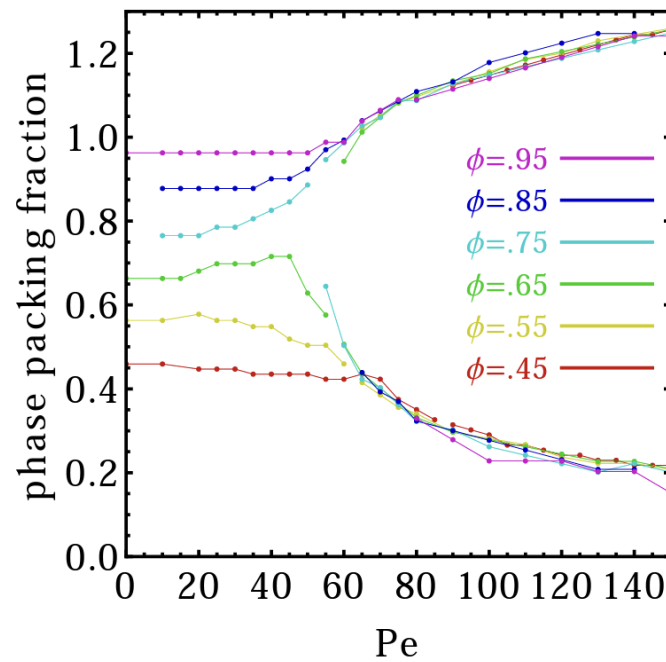
System spontaneously phase separates without attraction!

Controlled by Peclet number:

$Pe = \text{Persistence distance} / \text{diffusive distance}$



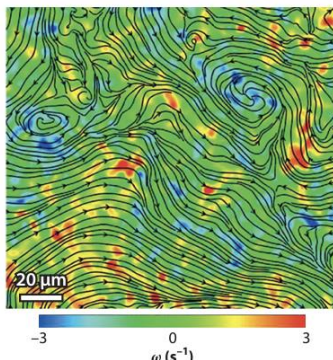
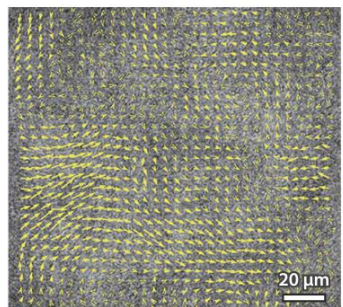
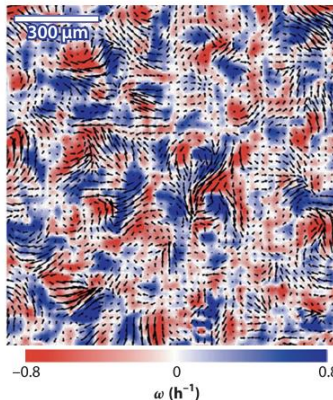
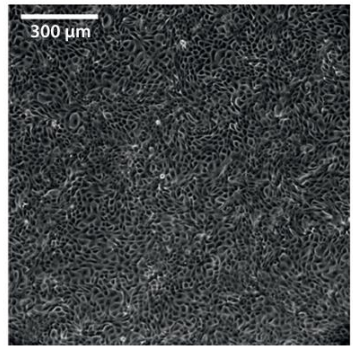
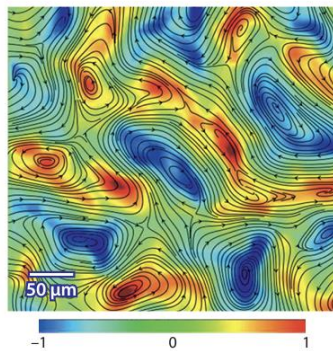
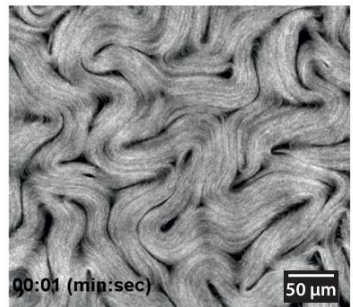
$$Pe = \frac{v_0}{D_r R}$$



G. Redner et al, Phys.
Rev. Lett. 110,
055701 (2013)

Experimental image

Vorticity field

d Bacterial suspension (*E. coli*, 3D)**e** Tissue cell monolayers**f** Microtubule-kinesin suspension (2D)

Classes of active turbulence,
Alert and Joanny 2022

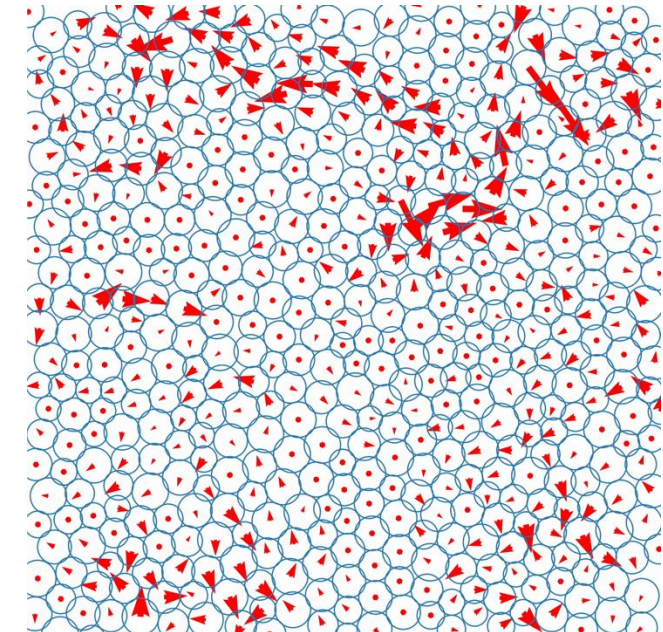
Cell sheet correlations and active turbulence

- ‘Swirly’ spatiotemporal correlation patterns, first reported by Trepat and Angelini, in MDCK cells
- Interpreted within the framework of nematic active liquid crystals and their turbulence / energy spectra (Yeomans, Giomi, many others).
- However, strongly resemble correlations seen in ABP glasses and dense fluids, and also sheared passive materials.

➤ Importance of active fluctuations

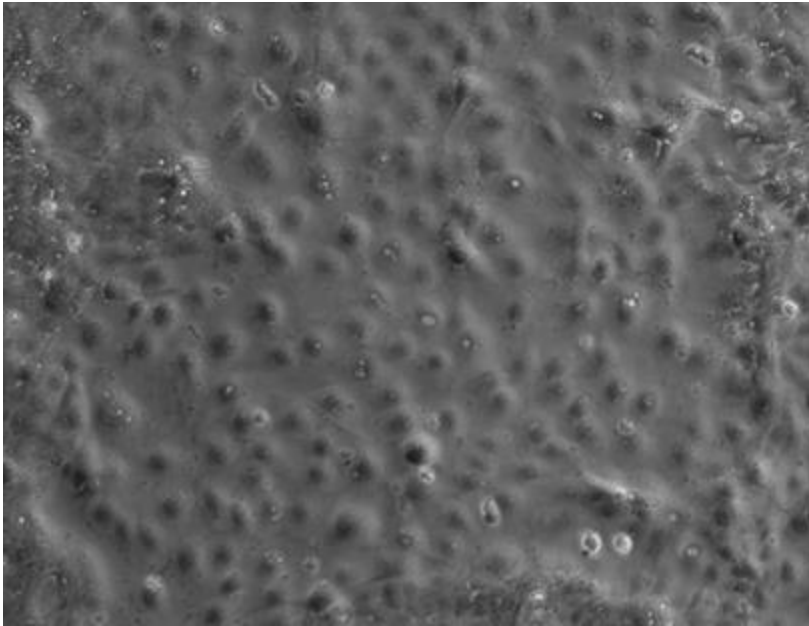
Microscopic null model of cell sheets: Uncorrelated crawling.
Nematic effects from cell-cell active stresses and cell shapes and are *additional*.

Excellent match without any of these effects 😊



ABP dense liquid

Experimental cell dynamics



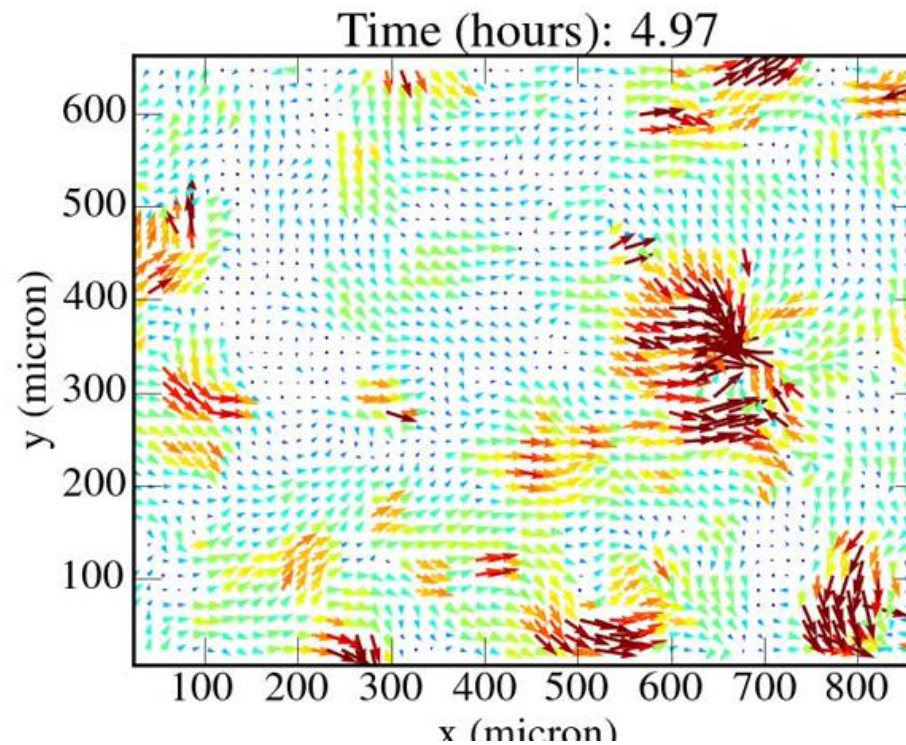
Kaja Kostanjevec

In vitro HCE (human corneal epithelial) cells on a substrate.

Measure

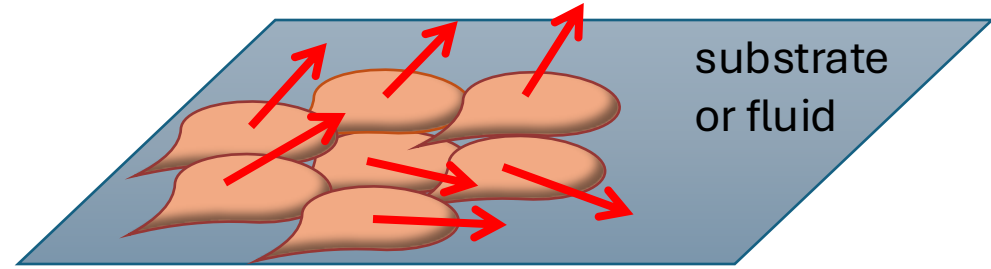
- Cell velocities and correlations
- Division and death rate

Migration patterns resemble other epithelial cell lines, e.g. in vitro MDCK



Use particle image velocimetry (PIV) to extract velocity fields.

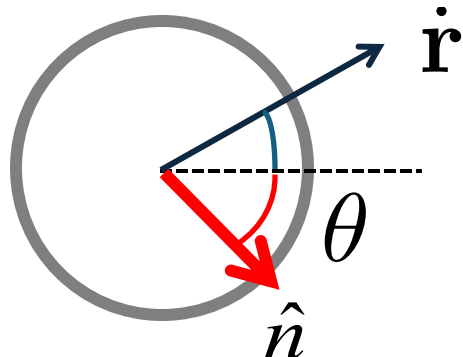
Persistent active driving and elasticity



Active Brownian dynamics:

$$\dot{r}_i = v_0 \hat{\mathbf{n}}_i + \frac{1}{\zeta} \sum_i \mathbf{F}_{ij}, \quad \dot{\theta}_i = \eta_i^r$$

$$\langle \eta_i^r(t) \eta_j^r(t') \rangle = 2D_r \delta_{ij} \delta(t - t')$$



Maps to a **time-correlated** active driving

$$\langle \hat{\mathbf{n}}_i(t) \cdot \hat{\mathbf{n}}_i(t') \rangle = e^{-|t-t'|/\tau}$$

Persistence time $\boxed{\tau = 1/D_r}$

Alternatively: Ornstein-Uhlenbeck driving

Lorentzian in frequency space, colored active noise:

$$\langle |\hat{\mathbf{n}}(q, \omega)|^2 \rangle = (2\pi)^3 \frac{2\tau a^2}{1 + (\tau\omega)^2}$$

Correlations in an active solid (1d)

Equation of motion of solid with modulus, for displacement field \mathbf{u} and velocity $\dot{\mathbf{u}}$

$$\ddot{\mathbf{u}} = v_0 \hat{\mathbf{n}} + \frac{K}{\zeta} \nabla^2 \mathbf{u}$$

In Fourier space:

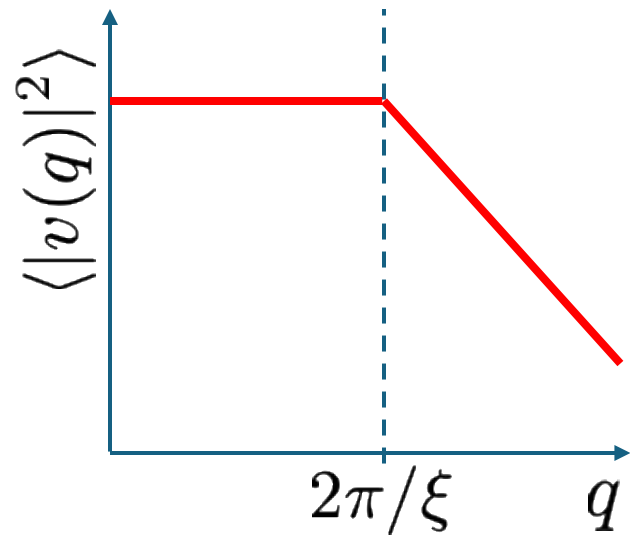
$$-i\omega \underbrace{\mathbf{u}}_{\mathbf{V}} = v_0 \hat{\mathbf{n}} - \frac{K}{\zeta} q^2 u$$

Spectra are convolution with colored active noise:

$$\langle |\mathbf{v}(q, \omega)|^2 \rangle = \frac{(2\pi)^3 \zeta^2 v_0^2 \tau \omega^2 a^2}{(K^2 q^4 + \zeta^2 \omega^2)(1 + (\tau \omega)^2)}$$

Integrate over frequency domain to find equal time correlation function:

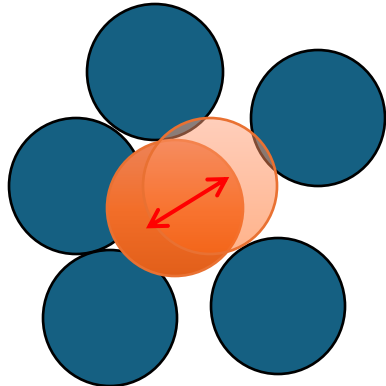
$$\langle |\mathbf{v}(q, t)|^2 \rangle = \frac{2\pi^2 v_0^2 a^2}{1 + K/\zeta \tau q^2}$$



Interacts with overdamped elasticity of solid with modulus K to generate **mesoscopic spatial correlations**.

$$\xi = \sqrt{\frac{K \tau}{\zeta}}$$

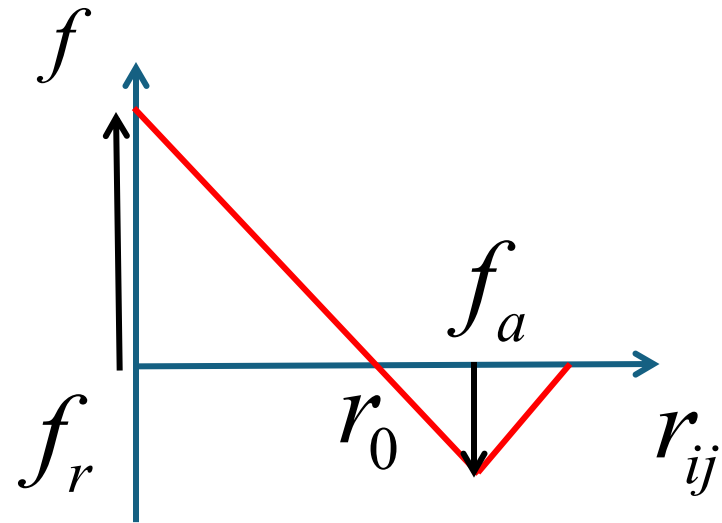
Add a (very) simple cell division model



*division
through fading-
in new particles*

- Implement constant death rate a , but density-dependent division rate

$$d = d_0 \left[1 - \frac{z}{z_{\max}} \right]$$



Model with only **three** scaled parameters, becomes tractable

d_0 bare division rate

$\frac{a}{d_0}$ ratio of death to division

$\frac{f_a}{f_r}$ ratio of attraction to repulsion

Obtain confluent self-melting state

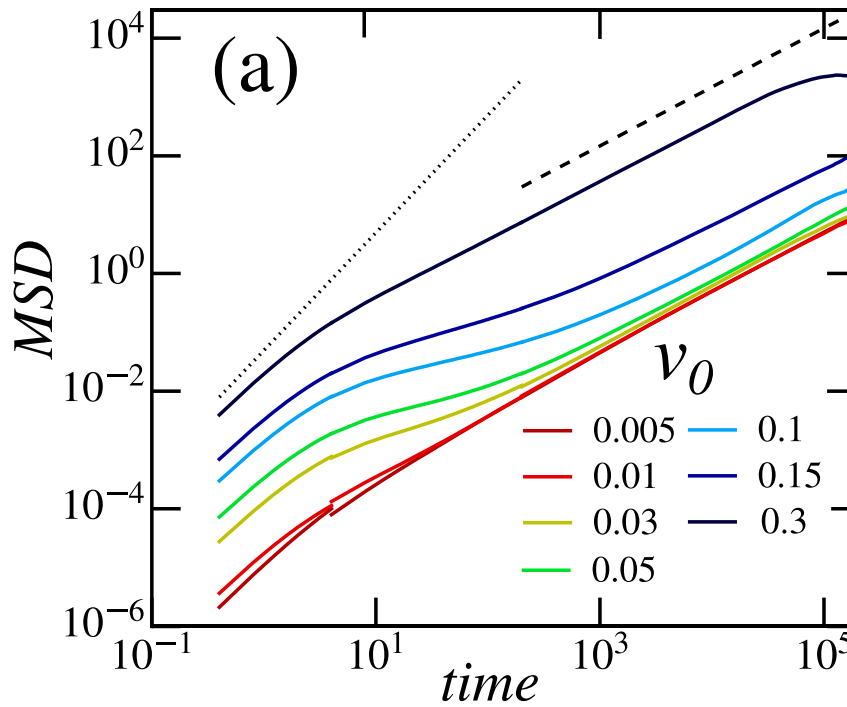
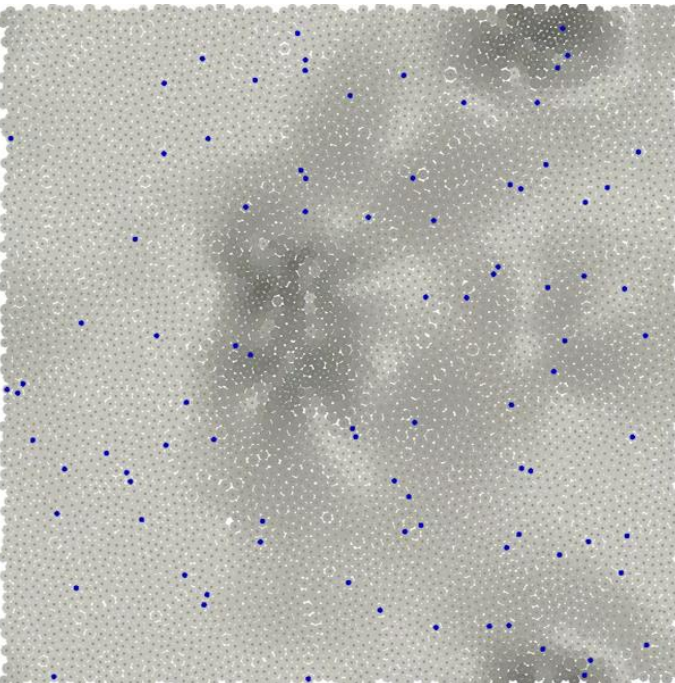
Not a glass: Any level of division results in fluid state (eventually)

$$\frac{\partial \rho}{\partial t} + \nabla \cdot (\rho \mathbf{v}) = (d(\rho) - a(\rho))\rho$$

Continuity equation: When growth and death terms are added, density is not conserved any more

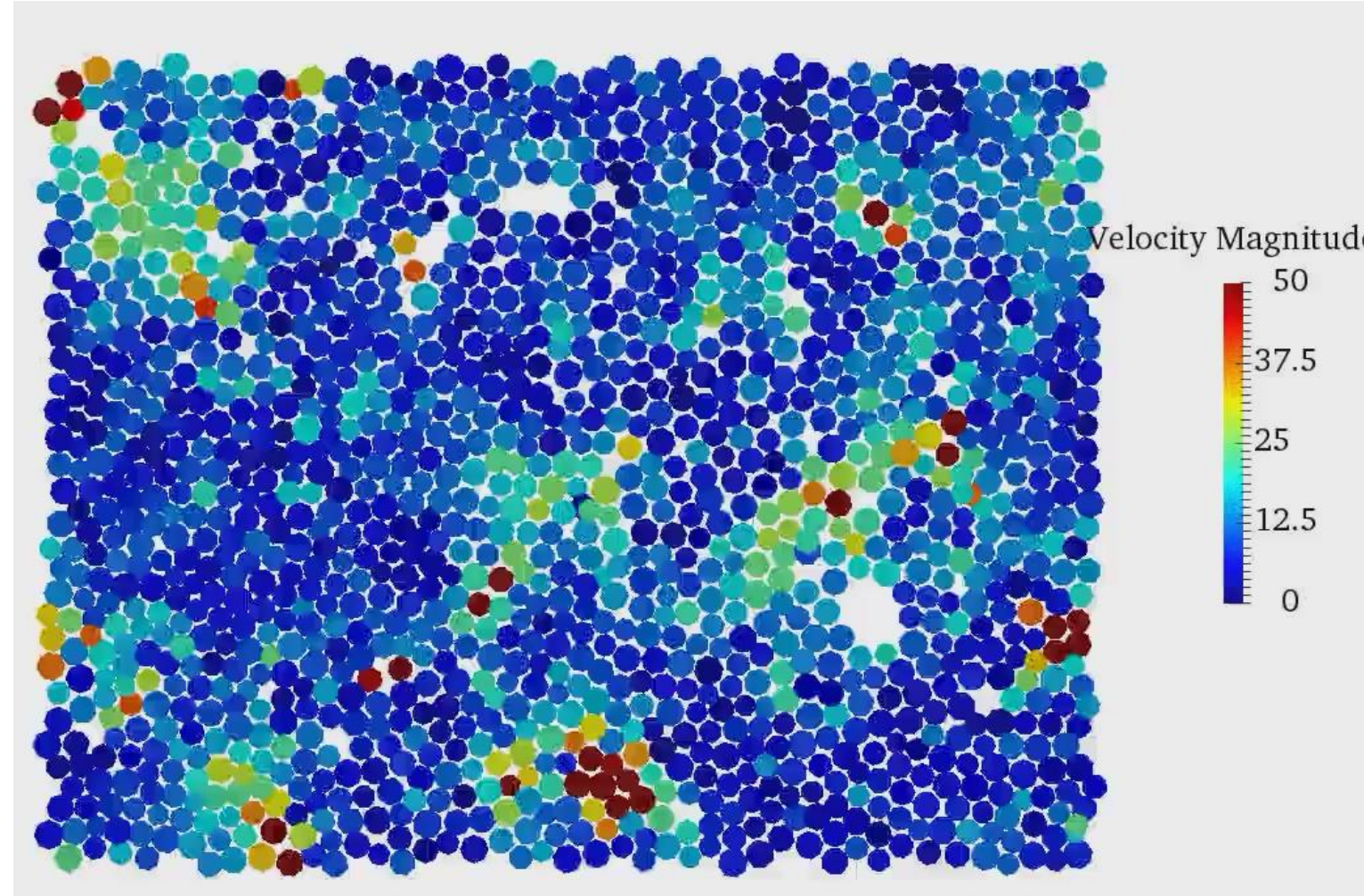
J. Ranft et al, PNAS, 107 (2010):

Continuum treatment shows the long-time diffusive behaviour with same time scale as ours



Develop fully parametrised simulations

Soft ABP disks + cell divisions



Parameters:

Cell radius R

Active velocity v_0

Rotational noise D_r

Potential stiffness k/ζ

Squeeze-out rate α

Ratio bare division to death $\frac{d_0}{\alpha}$

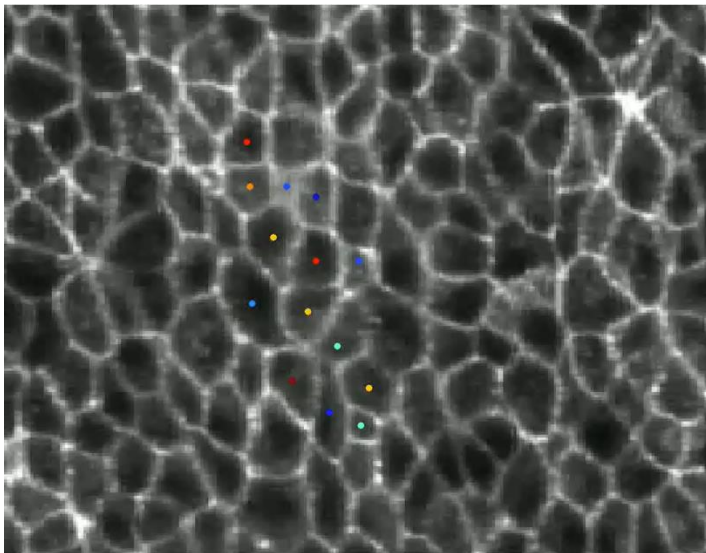
Next frontier:

Inferring cell-cell interactions
using machine learning (Chase Broedersz on Friday)

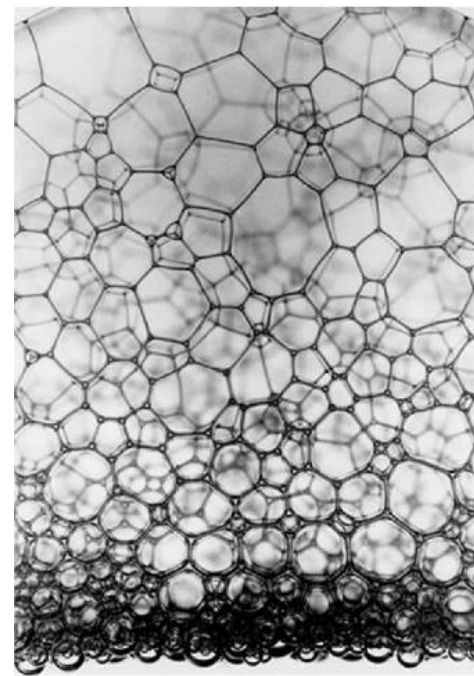
Outline: Making models of tissues

- I. Active Brownian particles: The simplest model – a demonstration
- II. **Vertex model with crawling activity: The self-propelled Voronoi (SPV) model**
- III. Vertex models with microscopic activity: Forces on junctions, and a zoo of new kinds of activity

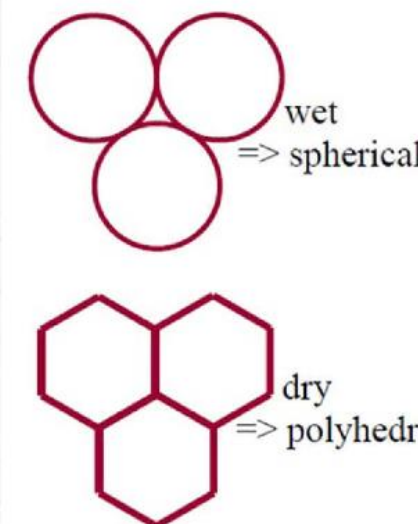
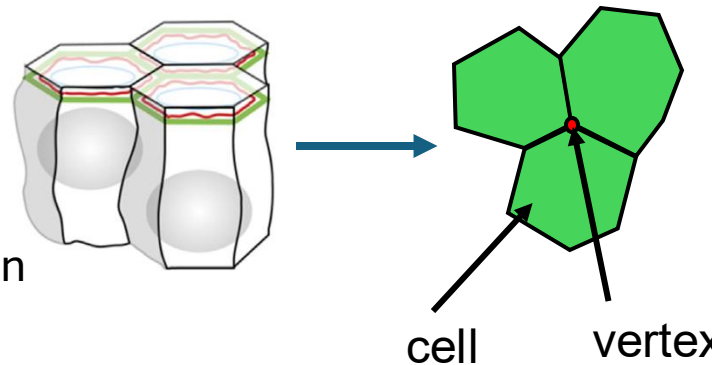
Microscopic model for realistic tissues?



movie courtesy of Antti Karjalainen
(Weijer group)



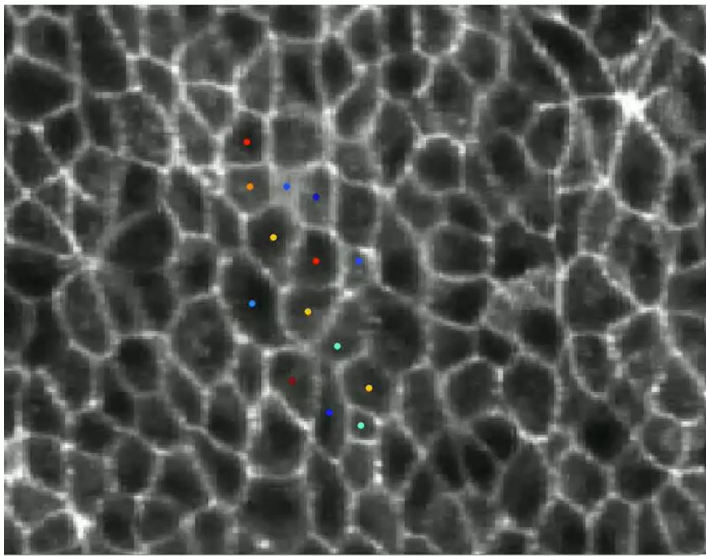
apical
actomyosin



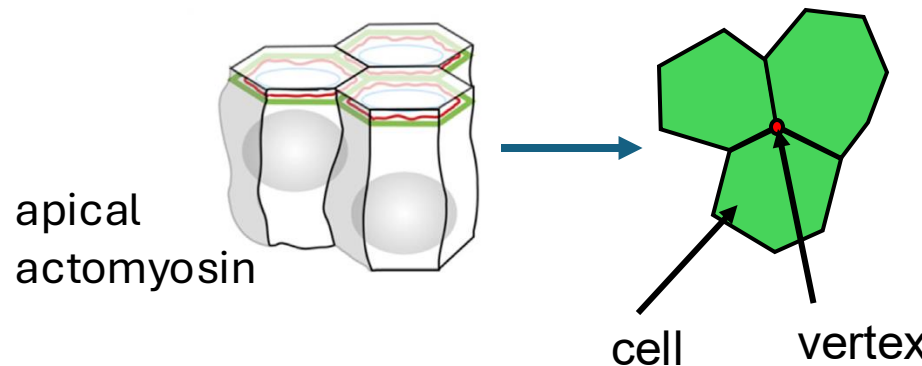
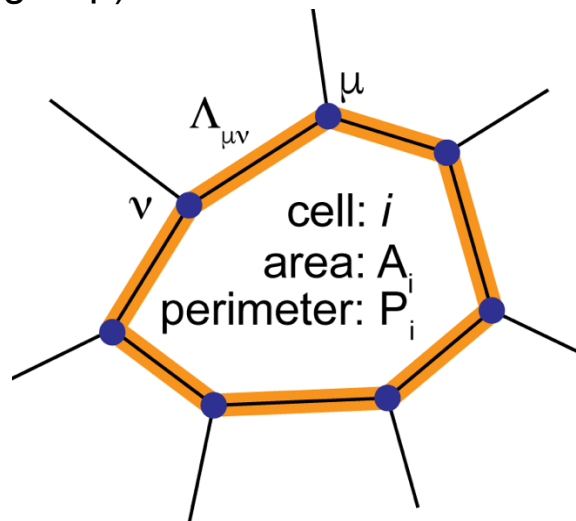
Looks very similar to the **physics of foams**:

In dry foams, bubbles directly share junctions with each other.
Shapes determined by surface tension and laplace pressure:
Minimise energy

Microscopic model for realistic tissues?



movie courtesy of Antti Karjalainen
(Weijer group)



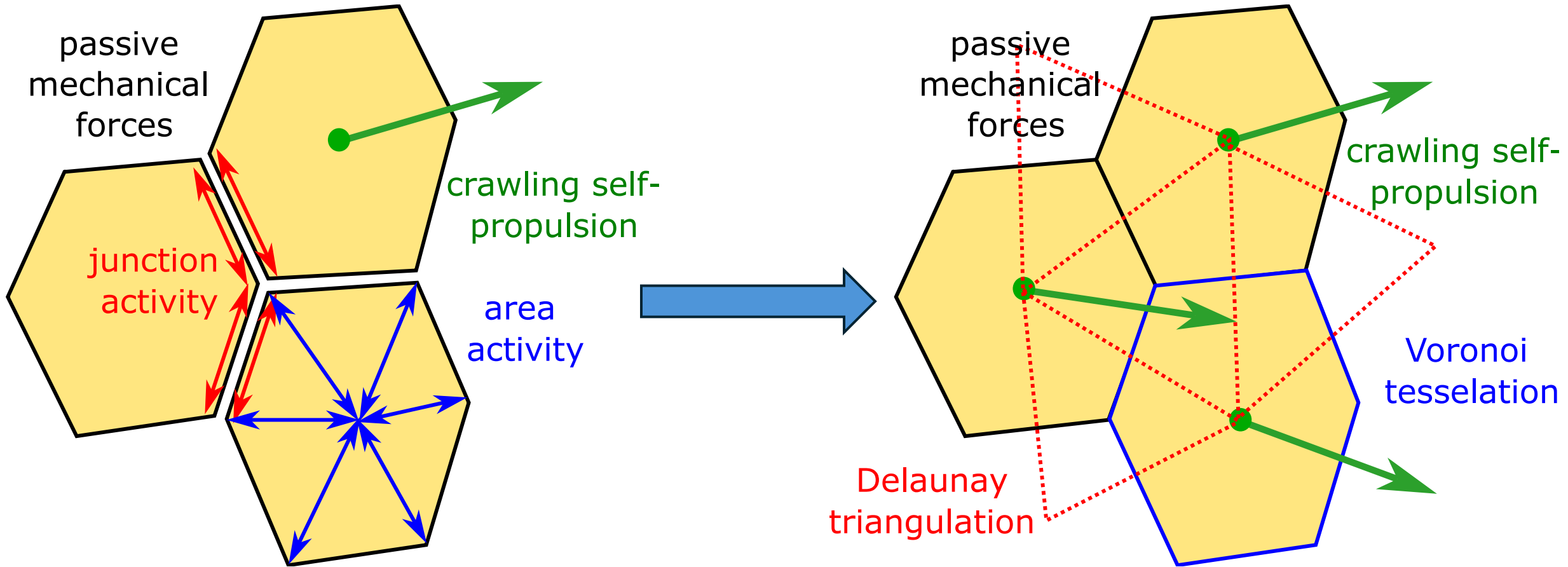
The Vertex model:

Nagai and Honda (1999), R. Farhadifar et al. (2007), A. Fletcher et al (2014)

$$V_{\text{Vertex}} = \sum_{i=1}^N \underbrace{\frac{\kappa}{2}(A_i - A_0)^2}_{\text{area change penalty (compressibility)}} + \underbrace{\frac{\Gamma}{2}(P_i - P_0)^2}_{\text{perimeter change penalty (contractility)}}$$

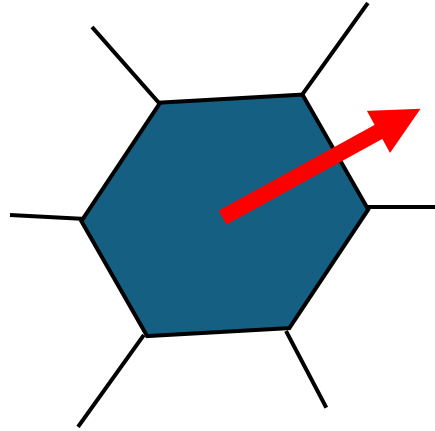
Originally: tissue conformation determined by energy minimisation.

Second approximation: The self-propelled Voronoi model



Self-propelled Voronoi model (SPV)

Add crawling active dynamics to the Vertex model:



Motility of the cell centres:

$$\dot{\mathbf{r}}_i = v_0 \hat{\mathbf{n}}_i - \mu \nabla_{\mathbf{r}_i} V_{\text{Vertex}}(\{\mathbf{r}_j\})$$

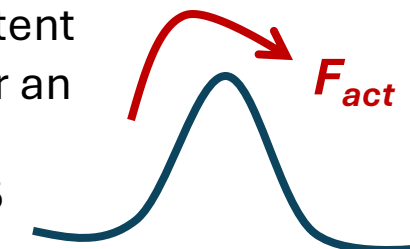
$$\dot{\phi} = \eta, \quad \langle \eta(t)\eta(t') \rangle = \frac{1}{\tau} \delta(t - t')$$

same as active Brownian particles

D. Bi et al, PRX 6, 021011 (2016)

Map between centres and vertices using a Delaunay triangulation / Voronoi tessellation

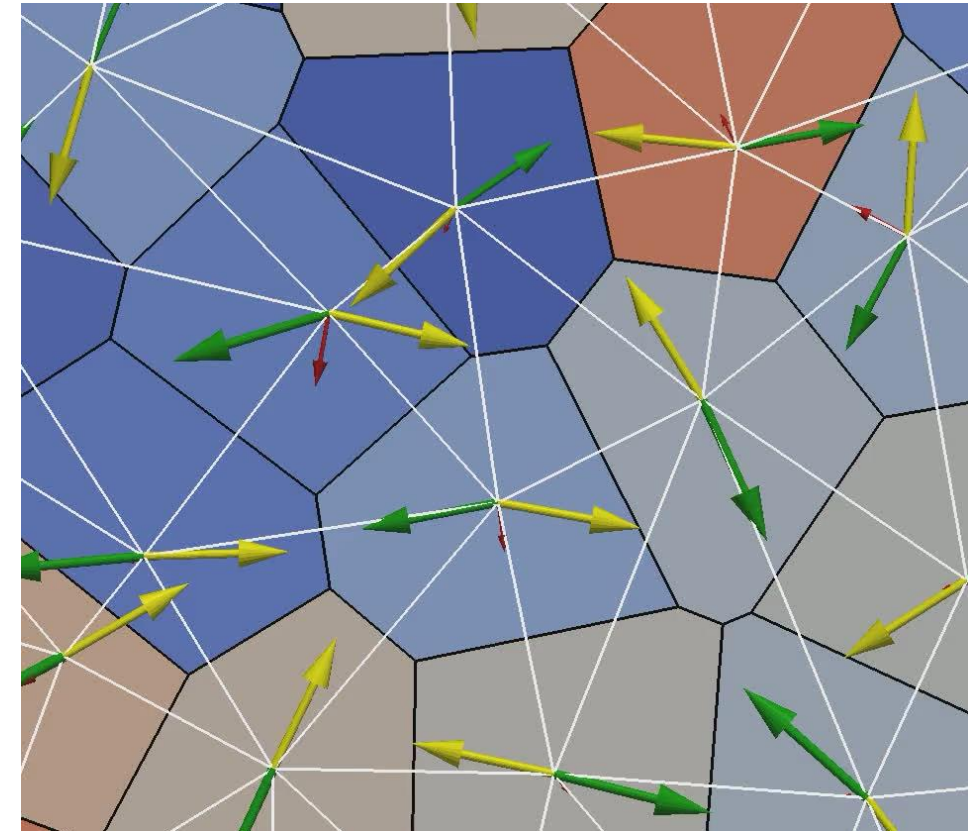
Slow contraction followed by fast expansion. Consistent with being dragged over an energy barrier
D. Bi et al, Nat. Phys. 2015



**T1 transitions:
cell rearrangements**

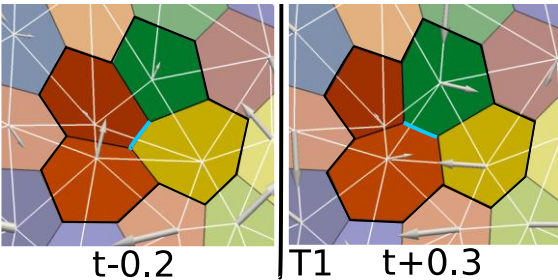
red: Cell centre velocity
green: active driving force
yellow: Conservative force from vertex model

Made using SAMoS, PLOS Comp. Biol. 2017



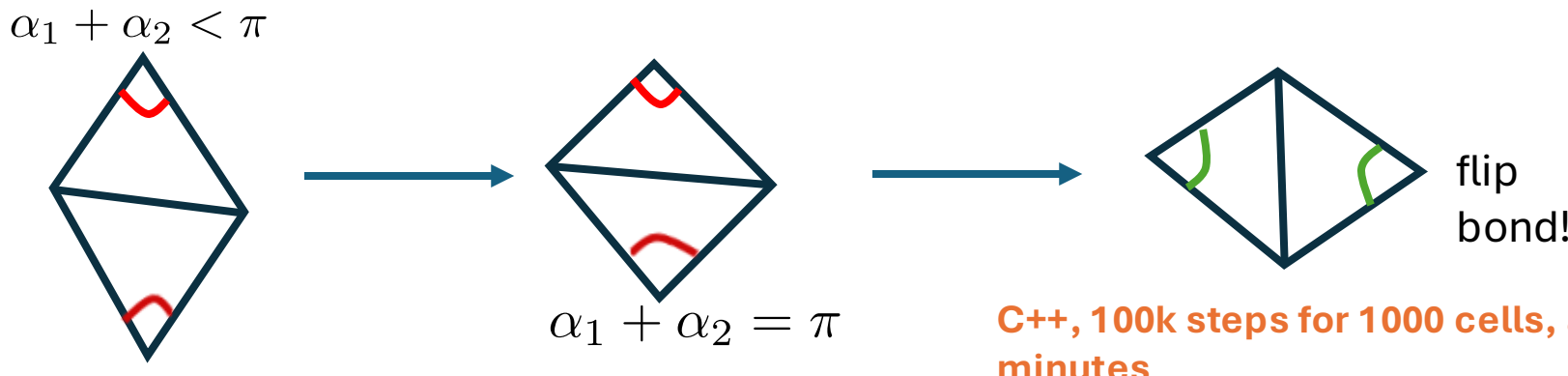
This is a hard problem!

- For a hybrid model (SPV) to work, we need a one-to-one and **continuous mapping** between vertices and cell centres.

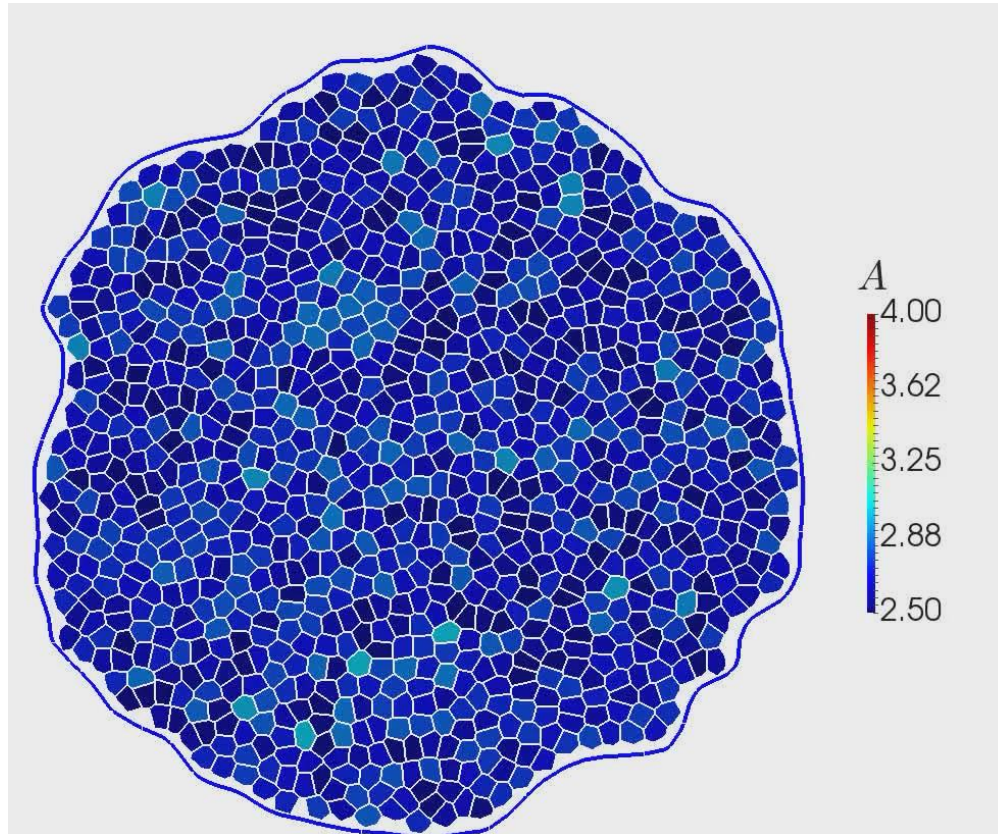


Otherwise, not a continuous energy function – no saddles, T1 events not resolved, does not equilibrate.

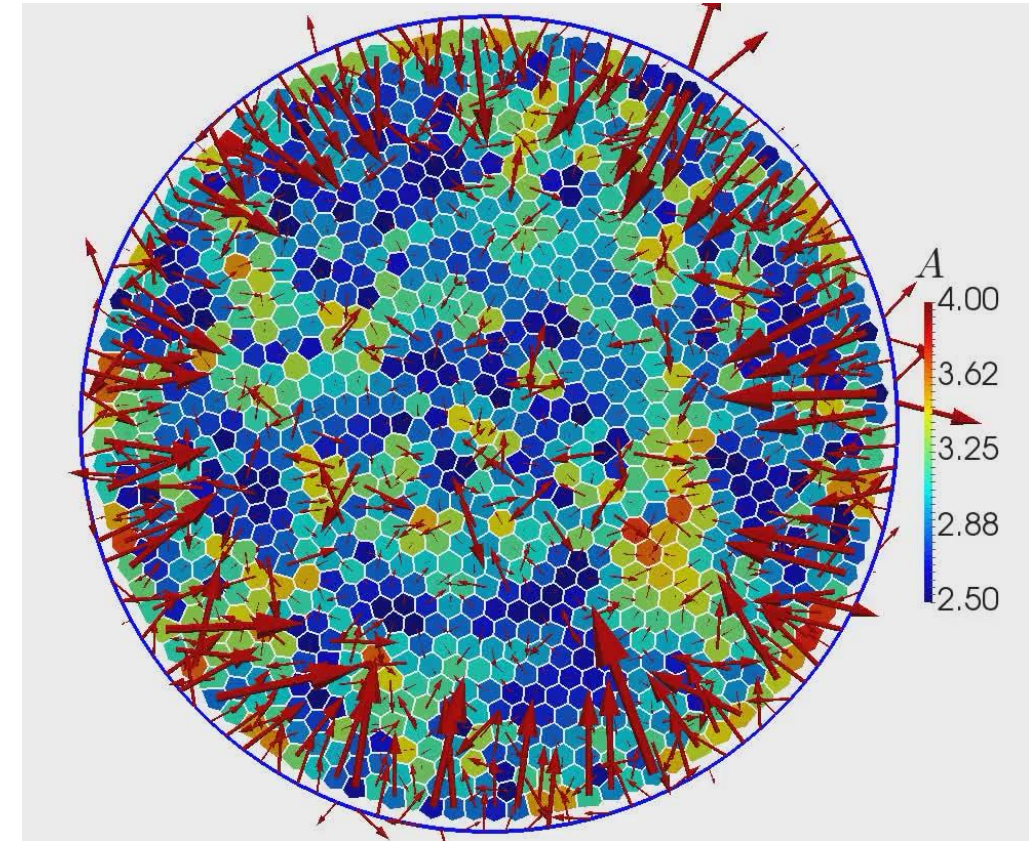
- The Delaunay triangulation / Voronoi tessellation is such a map (the only one?). However, it is **computationally expensive** to compute. Need to use tools from computational geometry to speed up.
- Final ingredients for an efficient algorithm:
 - Analytical computation of forces on cell centres through mapping between Delaunay circumcenters and Delaunay vertices
 - Edge flip to remain Delaunay triangulated at every step



Active solid / jamming transition



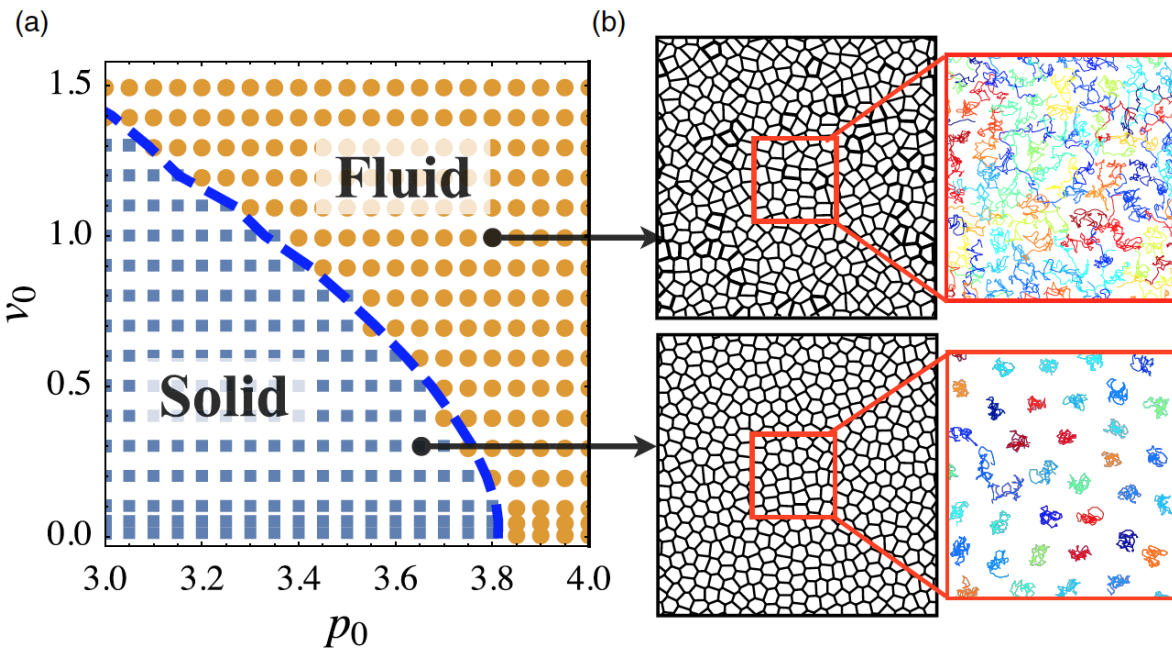
Liquid state: T1s and global flow



Solid state: No T1s, no global flow of the tissue

SAMoS implementation: D. Barton et al, PLOS Comp. Biol. 2017,
<https://github.com/sknepneklab/SAMoS>

Jamming / Glass transition in the SPV



D. Bi et al, PRX 6, 021011 (2016)

Can also melt the tissue with active driving, like for ABPs

Has features of a rigidity transition, one can use a version of Maxwell constraint counting for this model

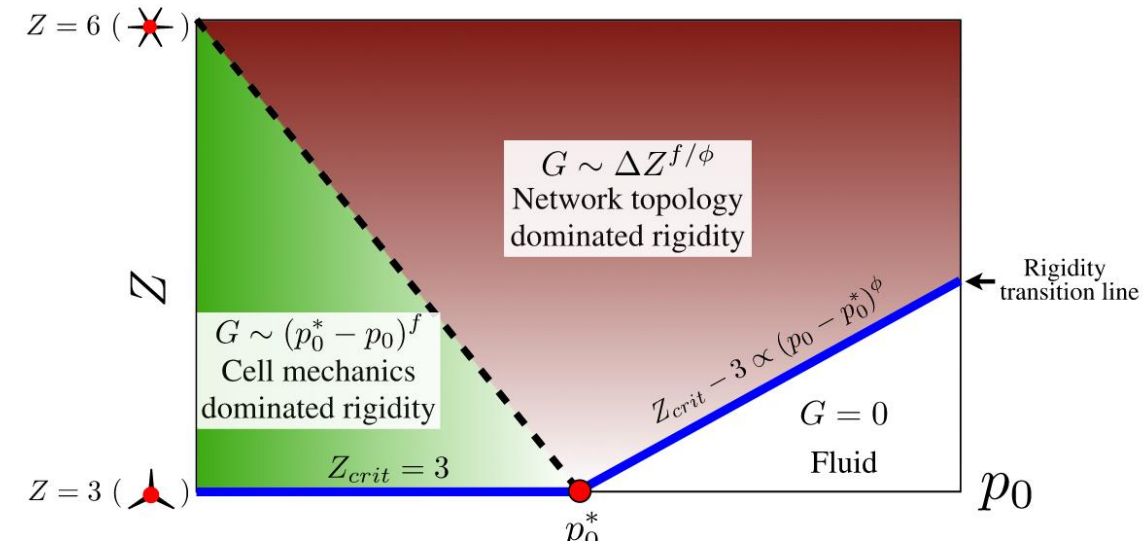
shape parameter $p_0 = \frac{P_0}{\sqrt{A_0}}$

3.72: regular hexagon

3.81: regular pentagon

4.0: regular square

Observe transition from solid to liquid at
 $p_0 \approx 3.81$

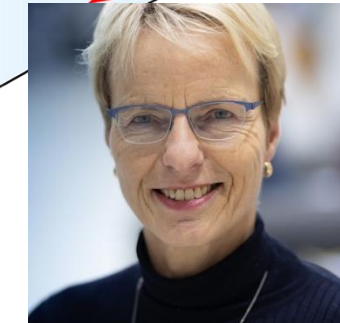
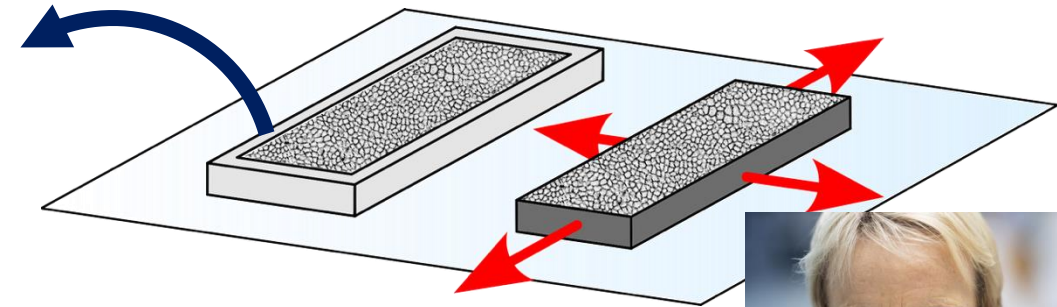


L. Yan and D. Bi, PRX 2019

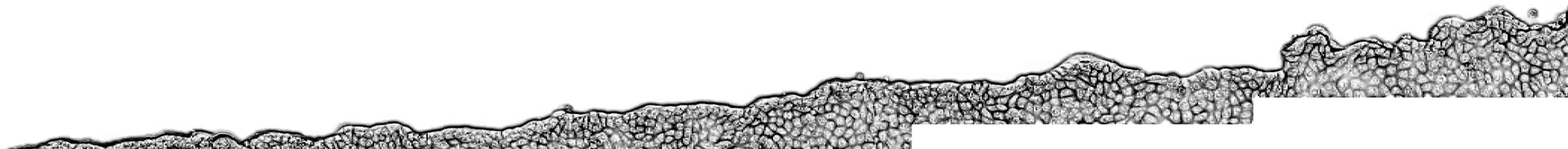
Epithelial finger formation



Sander Kammeraat



I. Näthke

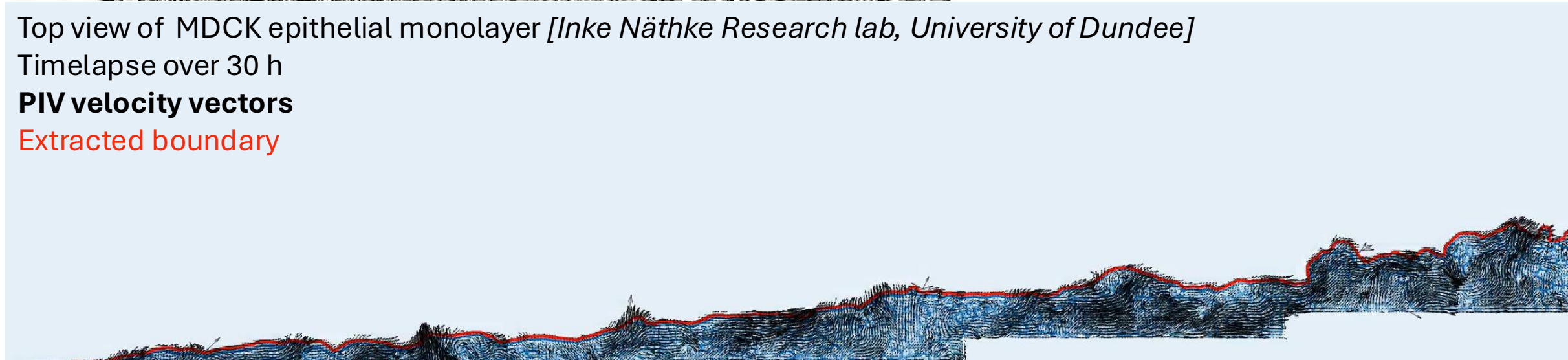


Top view of MDCK epithelial monolayer [*Inke Näthke Research lab, University of Dundee*]

Timelapse over 30 h

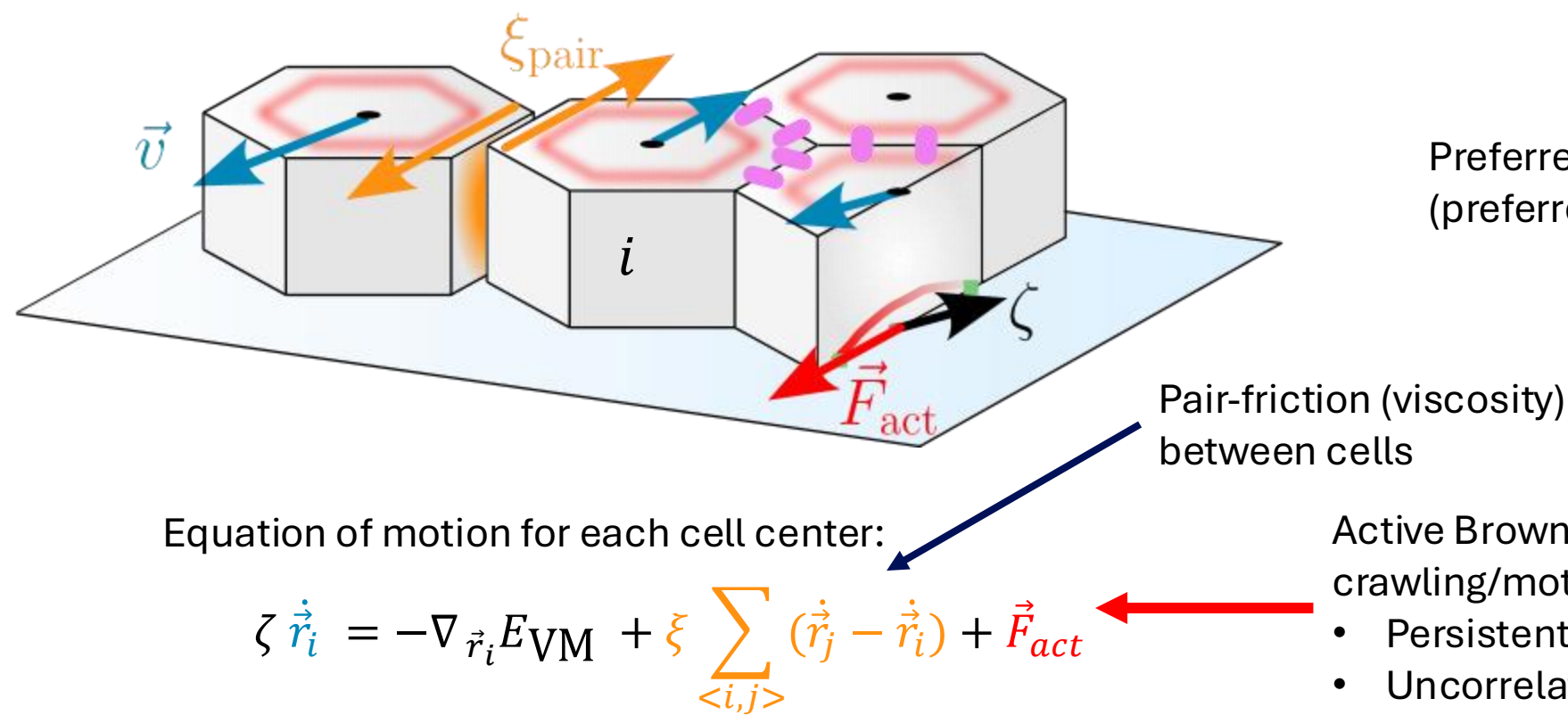
PIV velocity vectors

Extracted boundary



Self-propelled Voronoi sheet model

- In Voronoi models [Bi et al (2016) PRX]: positions of cell centers are the d.o.f.
- Shape of each cell determined by 2d Voronoi tiling



Each tiling has energy

$$E_{\text{VM}} = \sum_{i=1}^{N_{\text{cells}}} \frac{K}{2} (A_i - A_0)^2 + \frac{\Gamma}{2} (P_i - P_0)^2$$

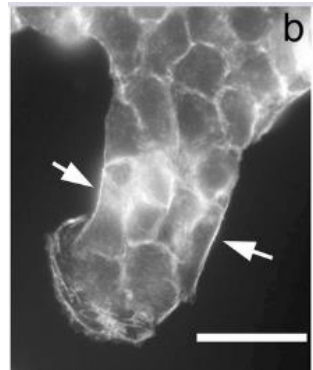
Preferred area
(preferred volume 2d)

Preferred perimeter
(Cell-cell adhesion & Cell contractility)

Active Brownian Particle activity (cell crawling/motility) with orientational diffusion D_r

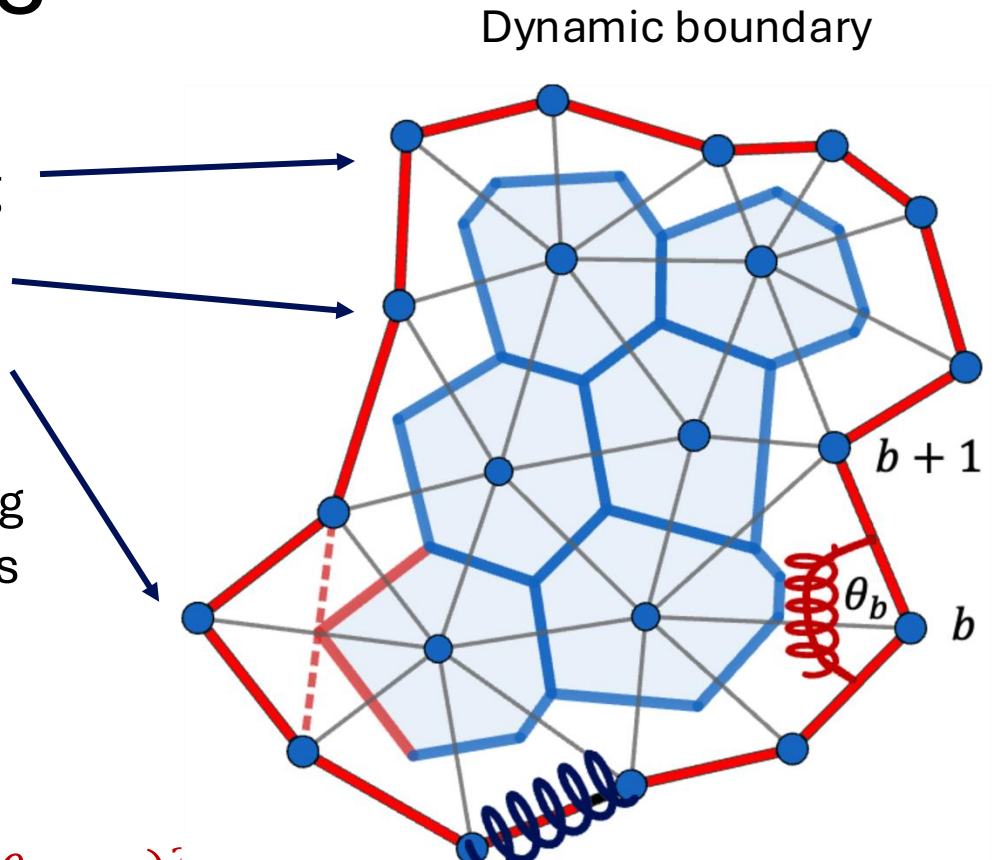
- Persistent in time
- Uncorrelated between cells

Modelling the actomyosin cable



[Poujade et al
(2007) PNAS]

- Boundary points needed to close Voronoi tiling can be used to model the actomyosin cable
- Boundary can grow/shrink by adding/removing these boundary points
- These boundary points have stretching/bending energy like coupled springs and angular springs



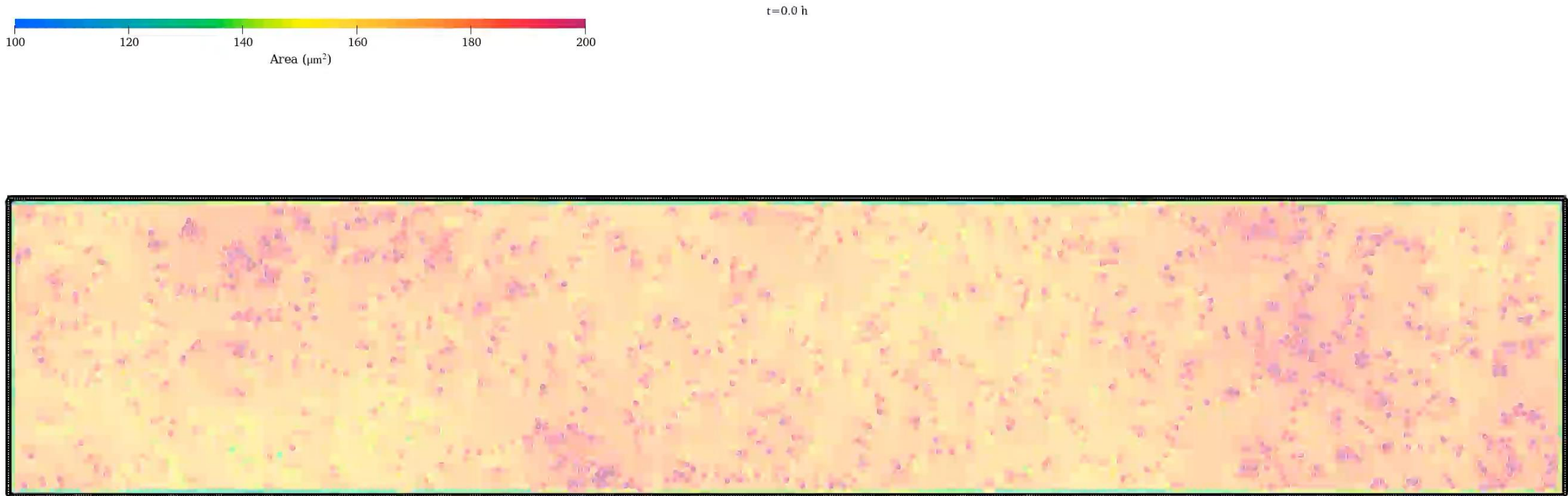
$$E_{AVM} = E_{VM} + \sum_{b=1}^{N_b} \left[\frac{k_s}{2} (l_{b,b+1} - l_0)^2 + \frac{k_b}{2} (\theta_b - \pi)^2 \right]$$

AVM and numerical implementation by Barton et al (2017) PLOS

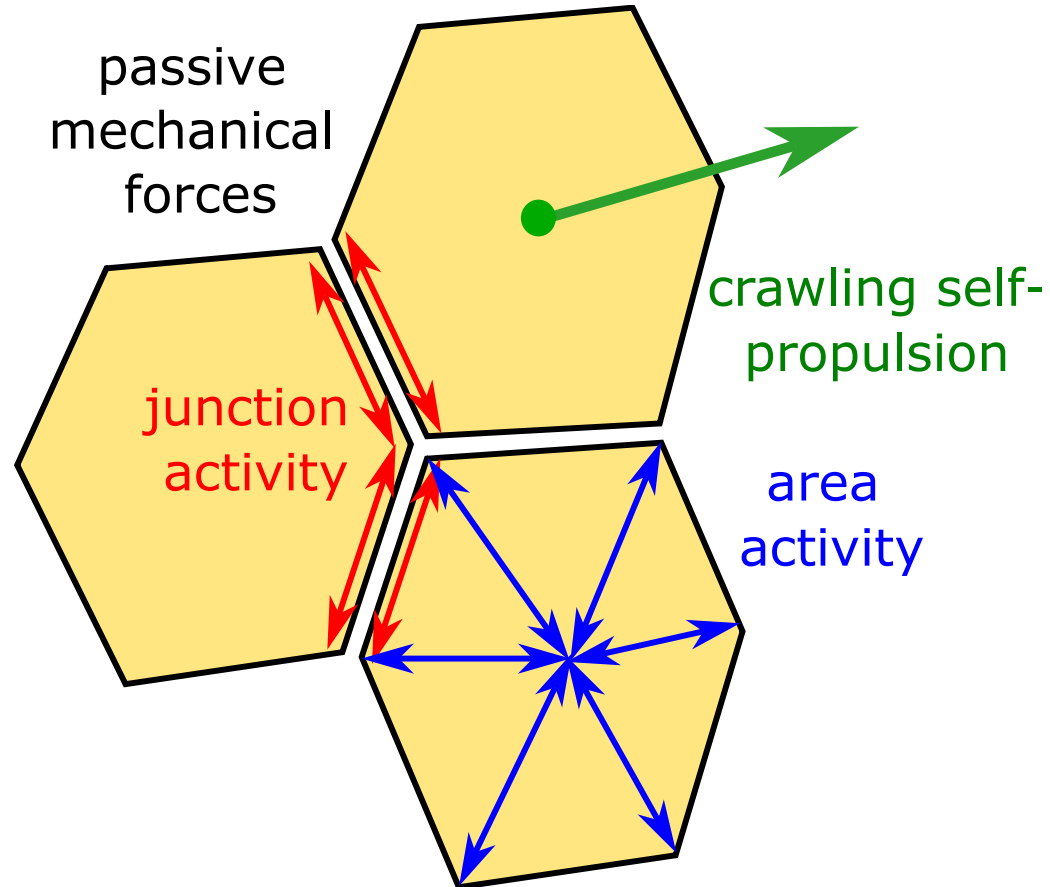


R. Sknepnek

Matched AVM simulations

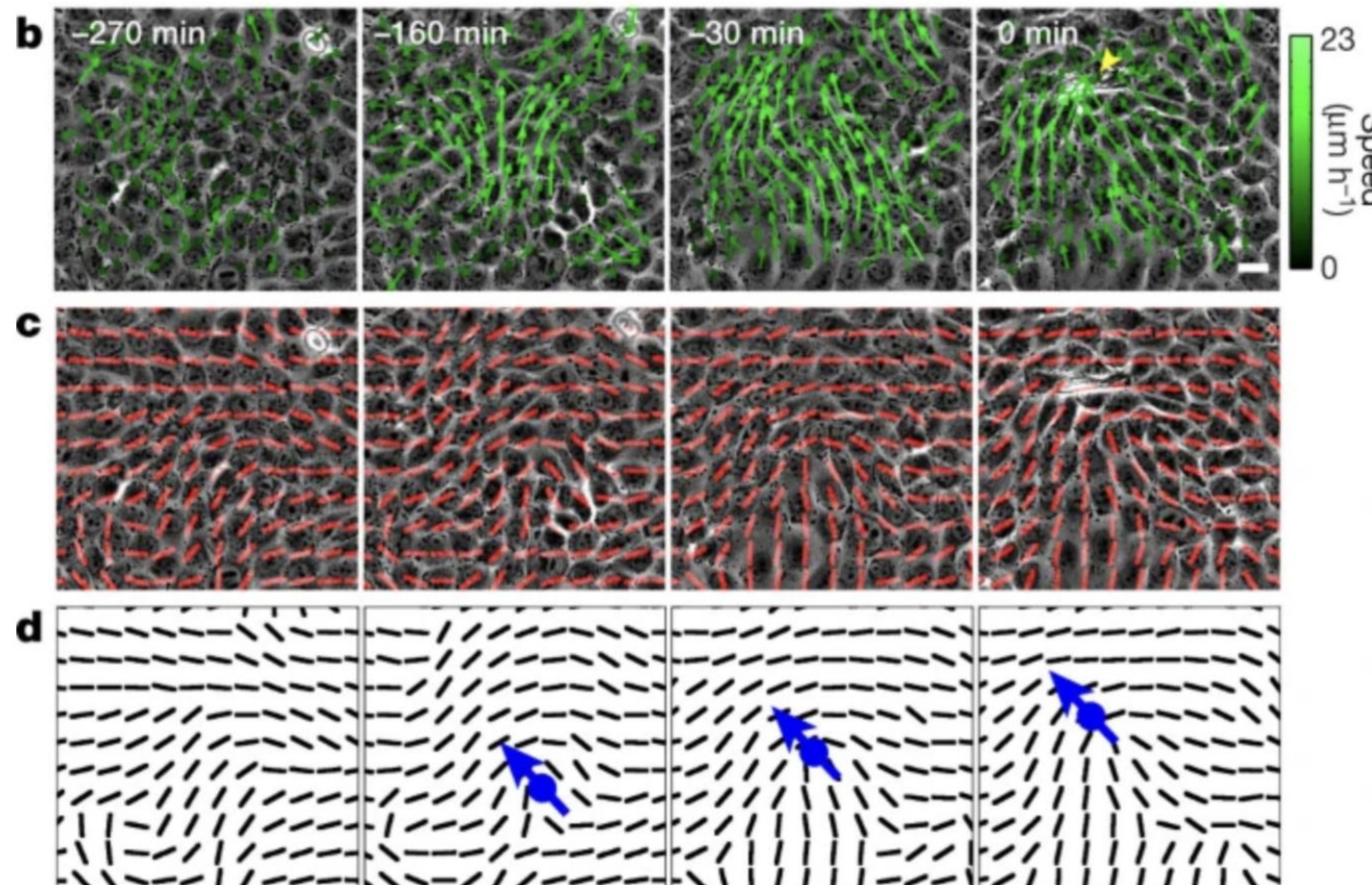


Third approximation: Vertex models with internal activity

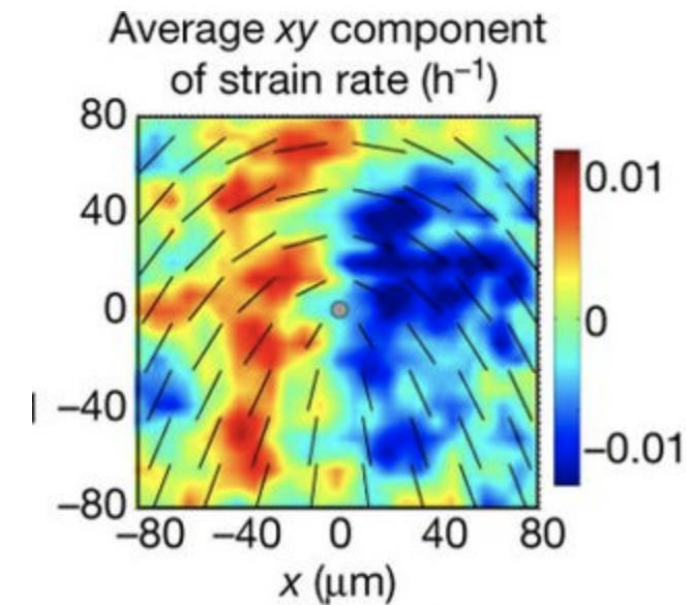


Active nematics and cell sheets

Observed: Active nematic properties with topological defects

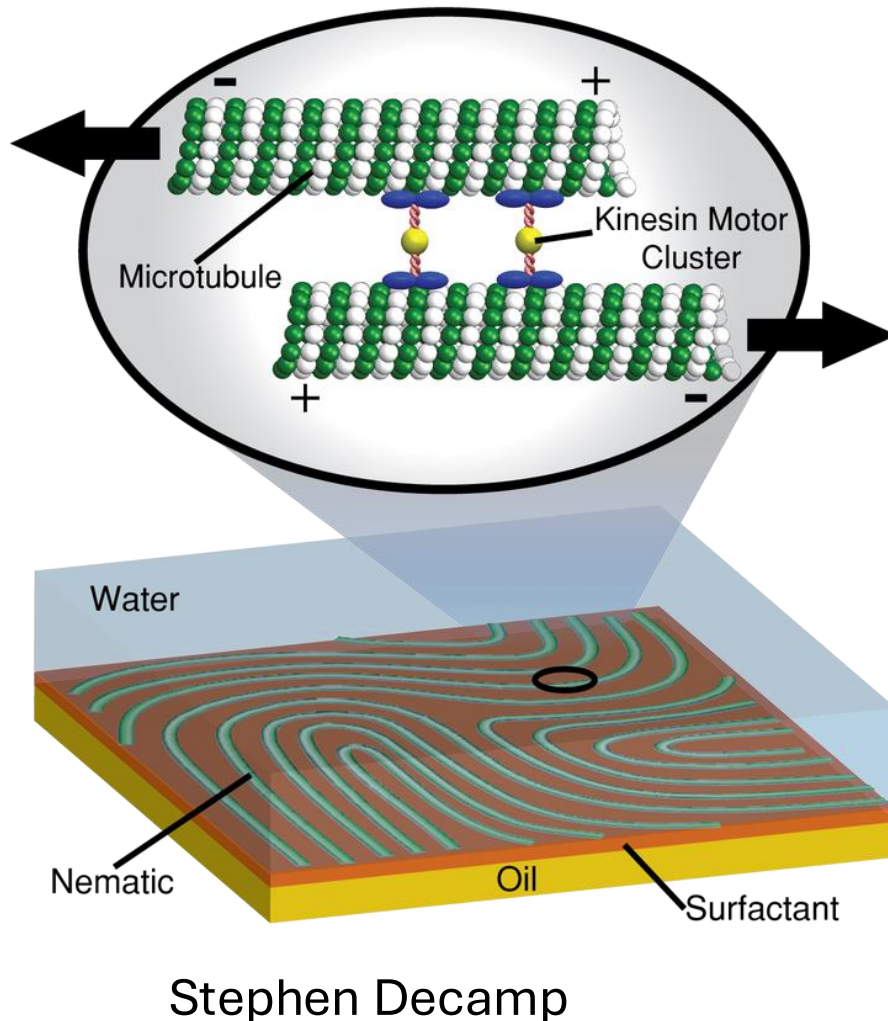


Moving +1/2 defects, and extrusion at +1/2 defects,
T. B. Saw et al, Nature 544, 212 (2017),
Balasumbramanian et al (2021)

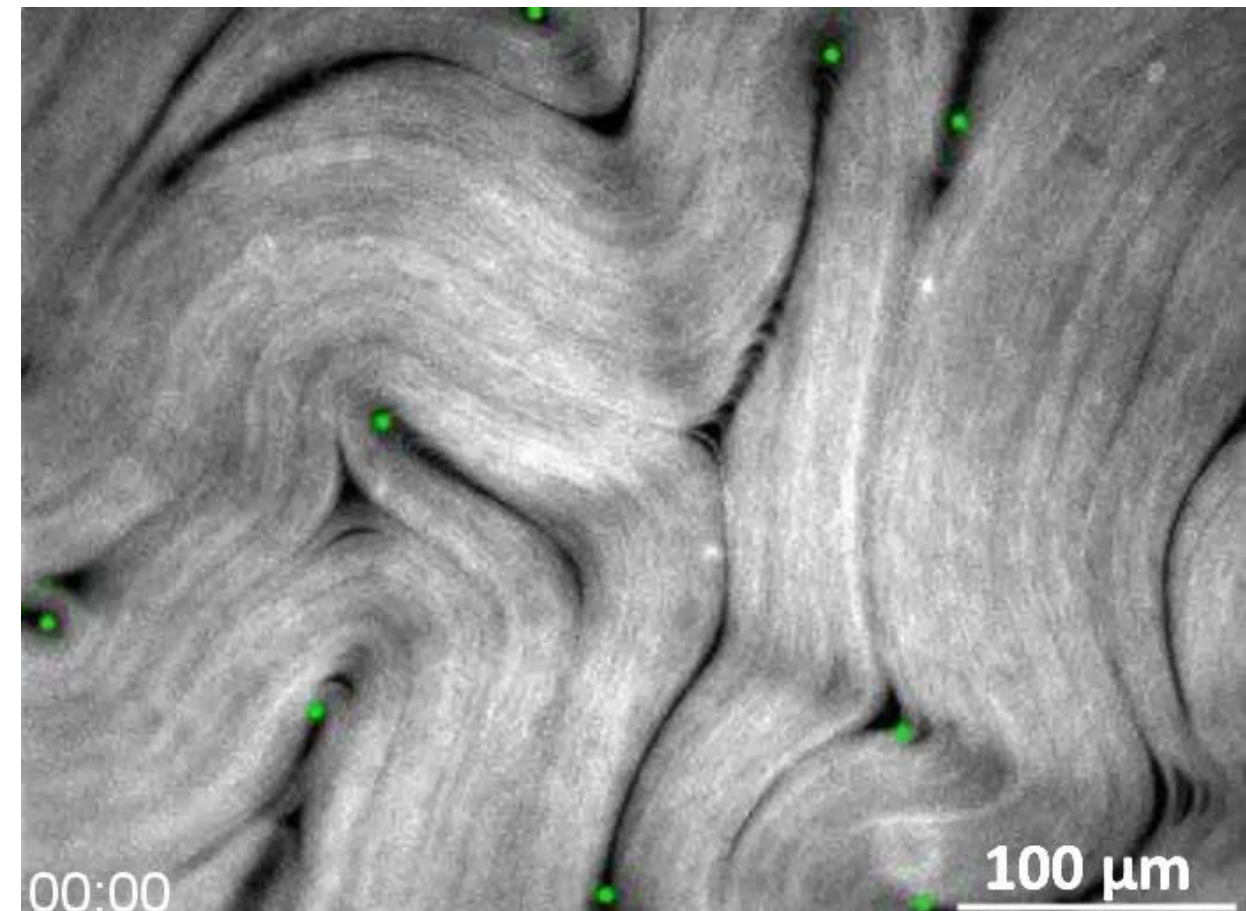


Active Nematics

(Luca Giomi on Thursday)

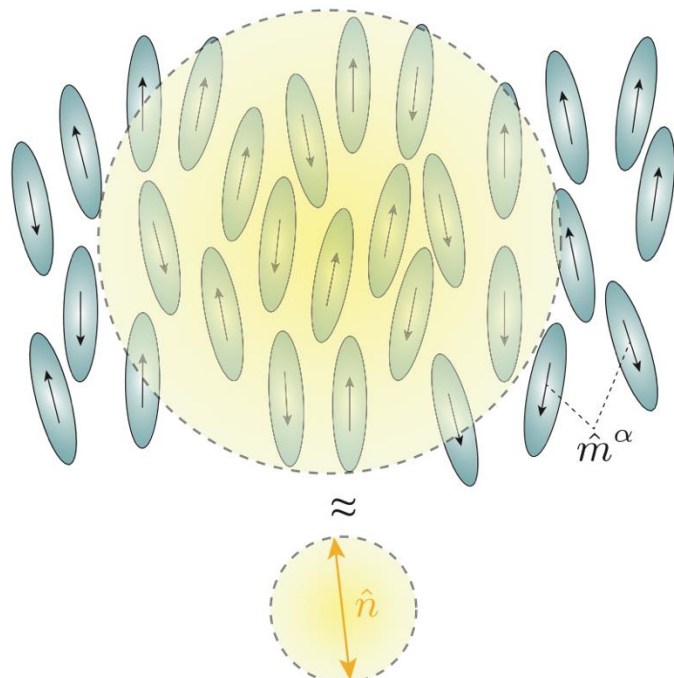


Classical example: bundles of microtubules with kinesin motors walking over them, confined to a 2d film.



group of Francesc Sagues

Nematic Liquid crystals



Consider a system of rod-shaped molecules pointing in unit directions \hat{m}_α , where we have the symmetry $\hat{m}_\alpha \leftrightarrow -\hat{m}_\alpha$

Construct symmetric, traceless tensor with that symmetry. Define nematic tensor field averaged over mesoscopic region V:

$$Q_{ij}^m = \frac{V}{N} \sum_\alpha \left(m_i^\alpha m_j^\alpha - \frac{1}{3} \delta_{ij} \right) \delta(\vec{r} - \vec{r}^\alpha)$$

Defines coarse-grained **nematic tensor** $Q_{ij} = \langle Q_{ij}^m \rangle$ with average nematic order strength S (between – and 1)

$$Q_{ij} = S \left(n_i n_j - \frac{1}{3} \delta_{ij} \right)$$

First example of a **hydrodynamic field** outside of fluids: Use Q to construct continuum models of liquid crystals, like we used ρ and v in fluid dynamics for the Navier Stokes equations.

Sketch of building hydrodynamic equations

First, find the correct hydrodynamic fields

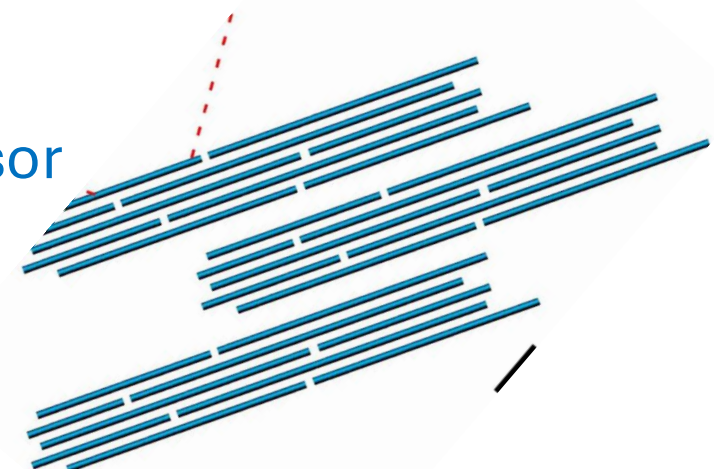
Second, write terms down allowed by symmetry

Convective derivative (Eulerian frame)

$$\frac{D A}{Dt} = \frac{\partial A}{\partial t} + \mathbf{v} \cdot \nabla A$$

$$\begin{aligned}\frac{Dc}{Dt} &= \text{concentration of active filaments} \\ \rho \frac{D\mathbf{v}_i}{Dt} &= \text{fluid flow velocity} \\ \frac{DQ_{ij}}{Dt} &= \text{nematic field, Q tensor}\end{aligned}$$

$$\hat{\mathbf{Q}} = \frac{1}{\rho(\mathbf{r}, t)} \int_0^{2\pi} \left(\hat{\mathbf{n}} \otimes \hat{\mathbf{n}} - \frac{1}{d} \mathbf{I} \right) p(\mathbf{r}, \theta, t) d\theta.$$



Sketch of building hydrodynamic equations

$$\frac{Dc}{Dt} = \partial_i \left[D_{ij} \partial_j c + \alpha_1 c^2 \partial_j Q_{ij} \right],$$

diffusion current

$$\rho \frac{Dv_i}{Dt} = \eta \nabla^2 v_i - \partial_i p + \partial_j \sigma_{ij}$$

viscosity stress tensor

$$\frac{DQ_{ij}}{Dt} = \lambda S u_{ij} + Q_{ik} \omega_{kj} - \omega_{ik} Q_{kj} + \frac{1}{\gamma} H_{ij},$$

flow alignment + rotation

Convective derivative (Eulerian frame)

$$\frac{D A}{Dt} = \frac{\partial A}{\partial t} + \mathbf{v} \cdot \nabla A$$

Diffusion dynamics of concentration of active filaments

Fluid flow dynamics = Navier-Stokes equation

Overdamped dynamics of nematic field

Variation of Landau-de Gennes free energy term:

$$H_{ij} = \frac{\delta F_{LG}}{\delta Q_{ij}}$$

Active instability

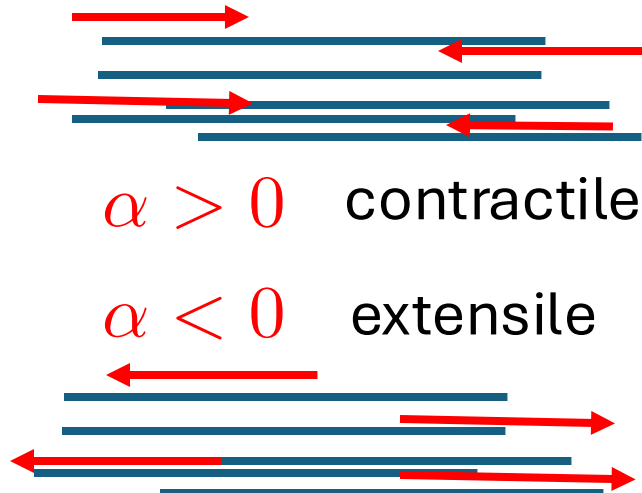
Stress tensor

$$\sigma_{ij} = -\lambda S H_{ij} + Q_{ik} H_{kj} - H_{ik} Q_{kj} + \alpha c^2 Q_{ij}$$

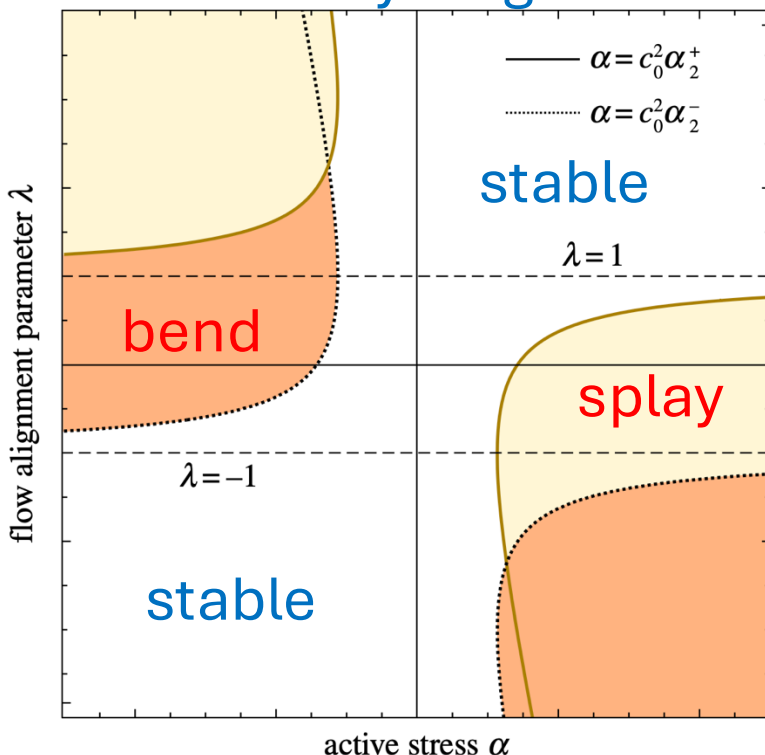
passive stress from nematic LC active stress

Steps:

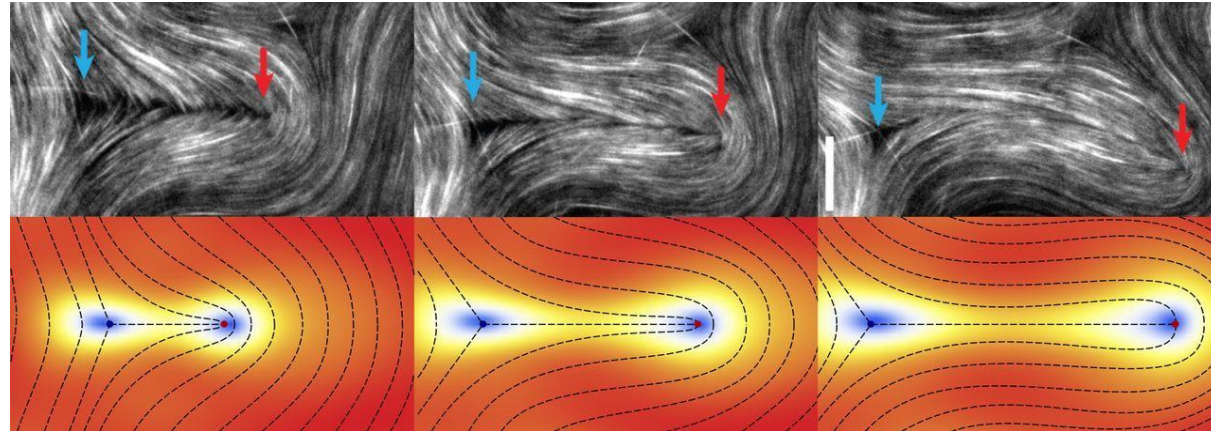
- Start from nematic state in free energy
- Linear stability analysis in Fourier space of coupled PDE equations
- Determine threshold for stability of the $q=0$ homogeneous state
- Bend instability for extensile activity (=this system), splay instability for contractile system



Stability diagram



Instability: spontaneous creation of defects

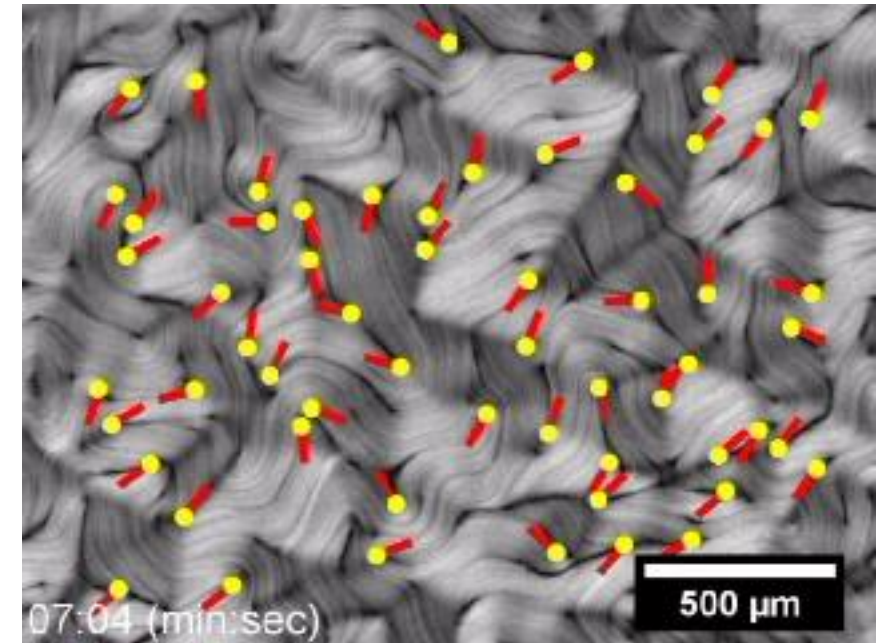


spontaneous formation of pairs of $+1/2$ and $-1/2$ defects

Bend instability followed by spontaneous forward motion of $+1/2$ defects, $-1/2$ defects are stationary.

Reason: different flow patterns around different defect states

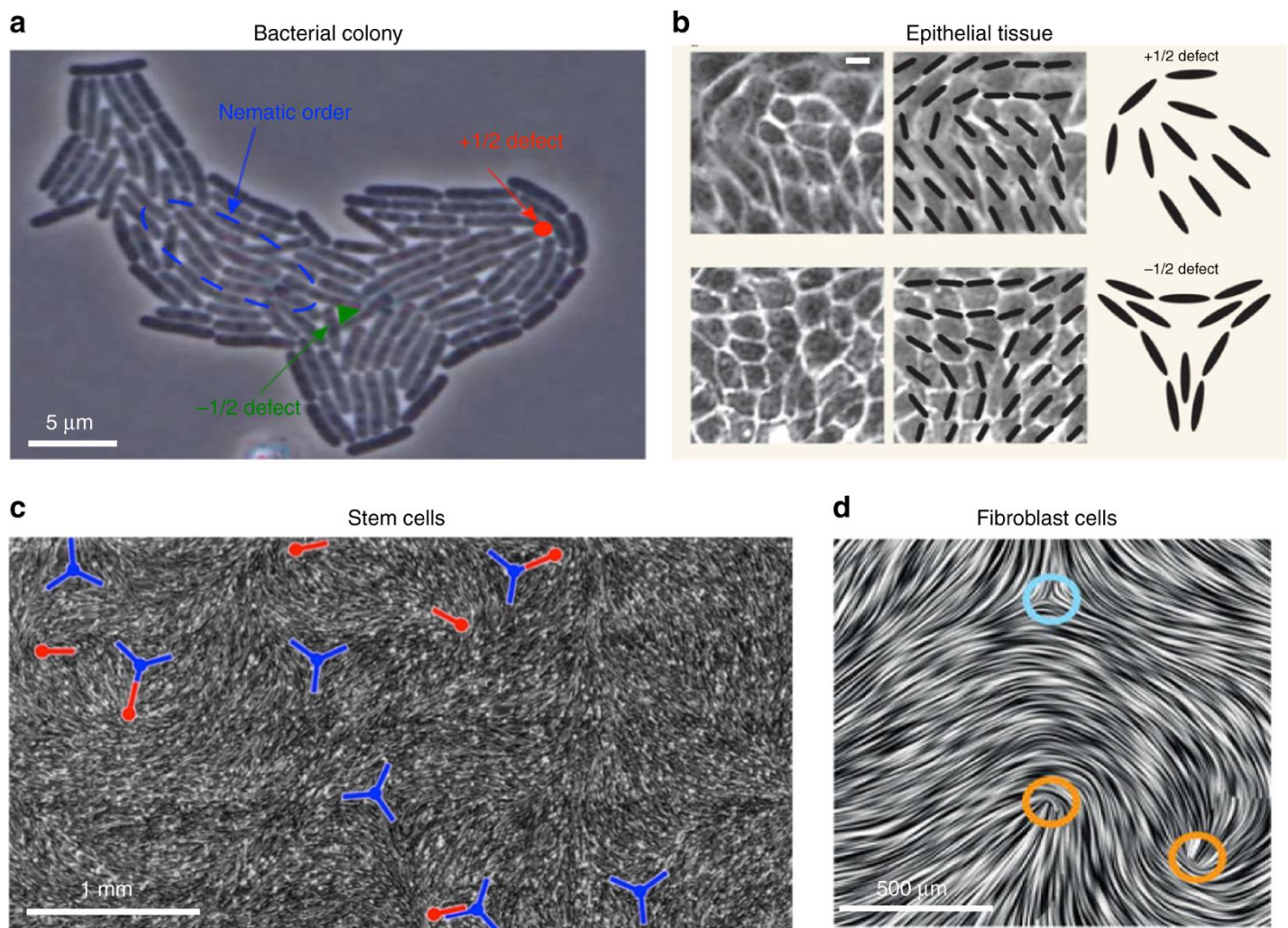
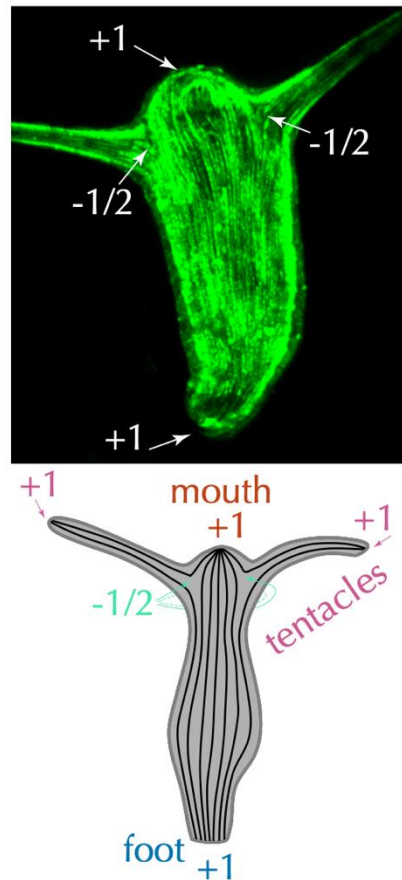
tracking defect motion



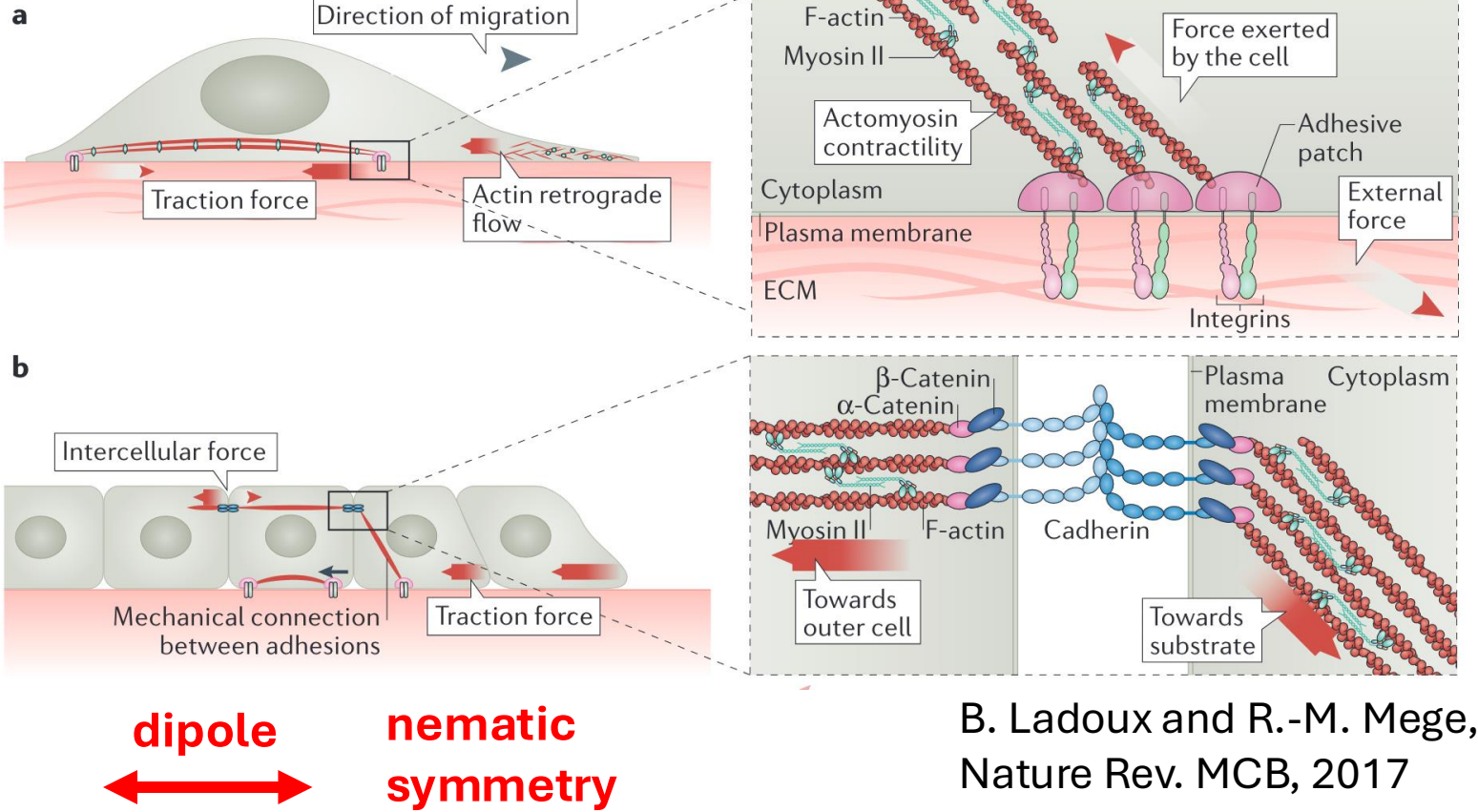
S. J. DeCamp et al, Nature Materials 14, 1110–1115 (2015)
(Z. Dogic group)

Biological examples of active nematics

Hydra: small, sea-anemone like



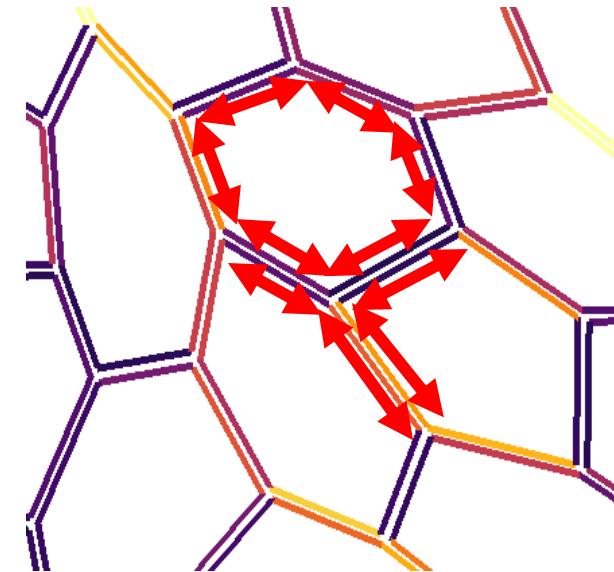
Miroscopic origin?



B. Ladoux and R.-M. Mege,
Nature Rev. MCB, 2017

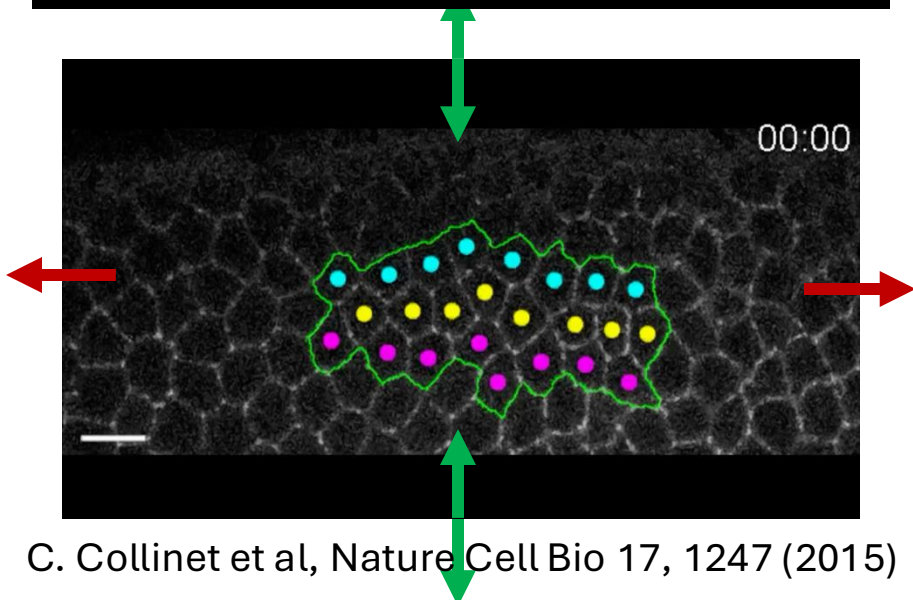
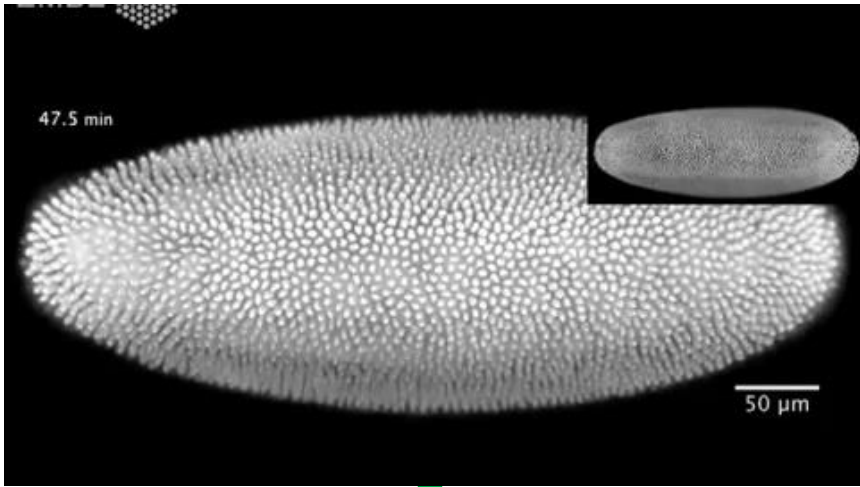


Nematic active stresses are generated by forces along junctions



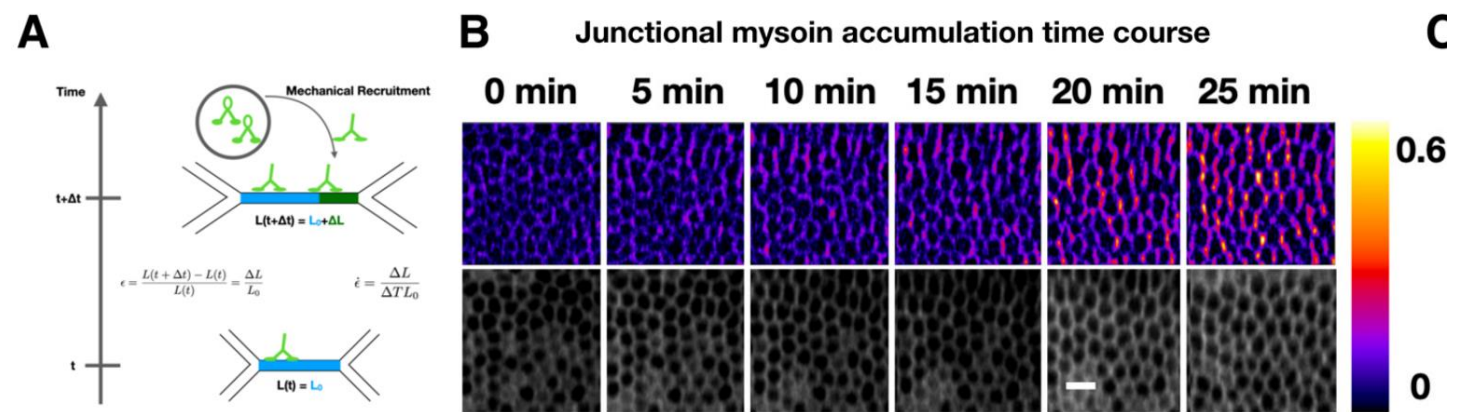
R Sknepnek, I Djafer-Cherif, CJ Weijer
and SH, Elife 12, e79862 (2023)

Developmental biology: Gastrulation



C. Collinet et al, Nature Cell Bio 17, 1247 (2015)

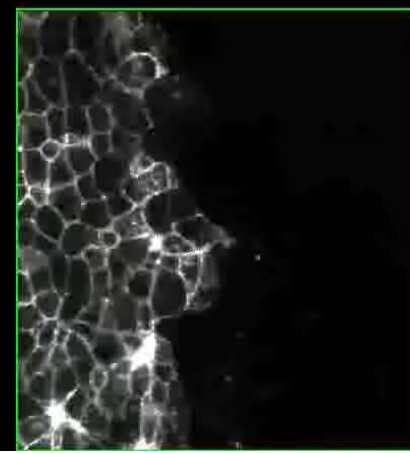
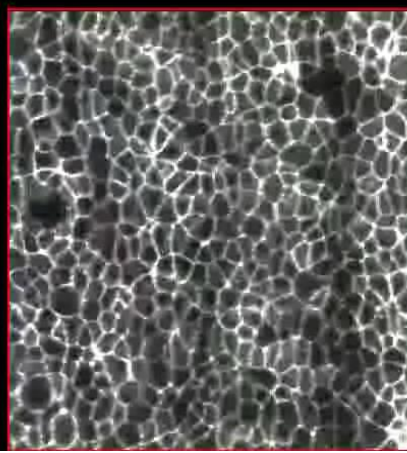
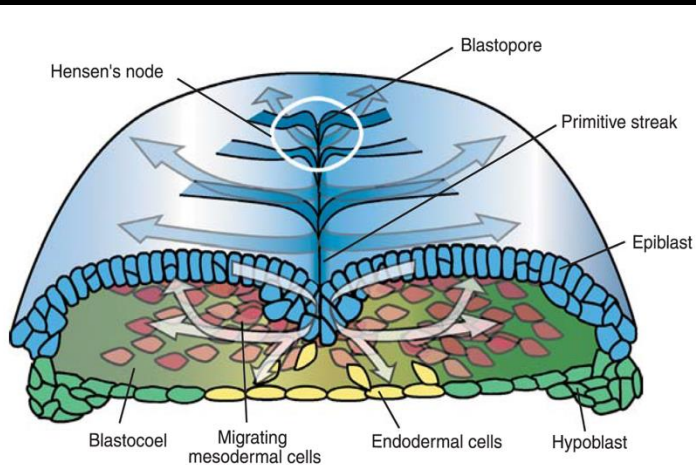
- Anisotropic Myosin accumulation along junctions, with mechanical feedback.
- Rearrangement along active T1 transitions, first seen in Drosophila germ band extension



H. Gustafson et al, Nat. Comm. 2022

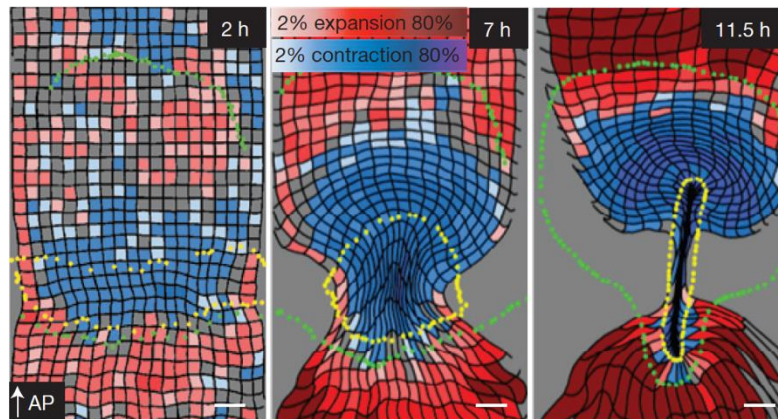
Primitive streak formation in the chick embryo

E. Rozbicki et al, Nat. Cell Biol. 17, 397–408 (2015)

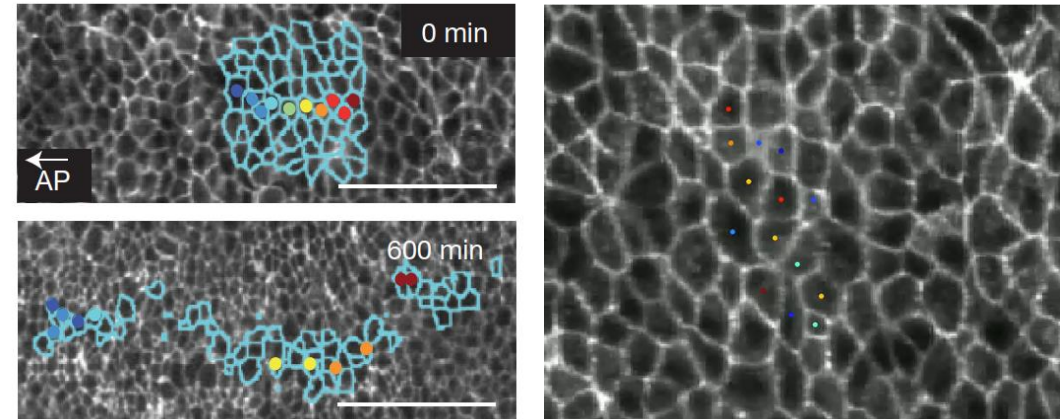


Junction-based activity leads to convergent extension

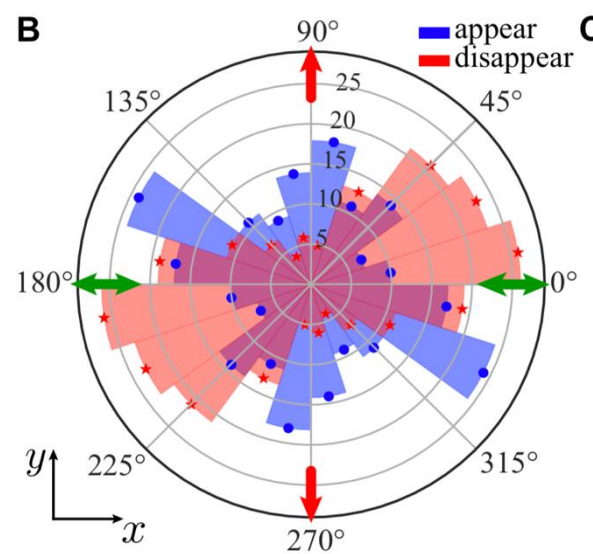
Global strain pattern: convergence-extension of sickle region into streak



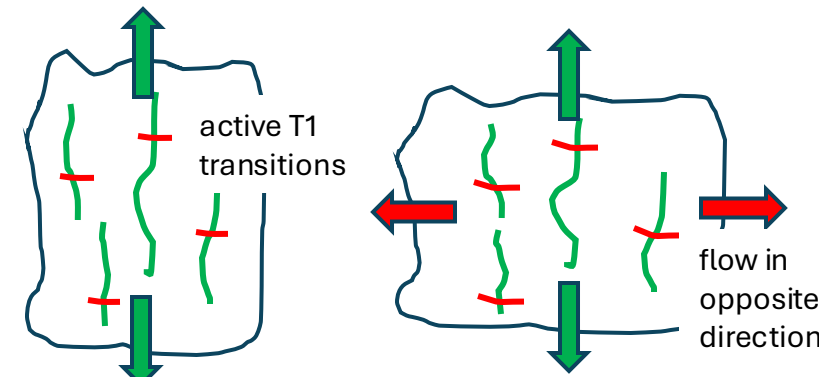
Local strain pattern: large amounts of rearrangements, divisions, ingestions, complex liquid rheology



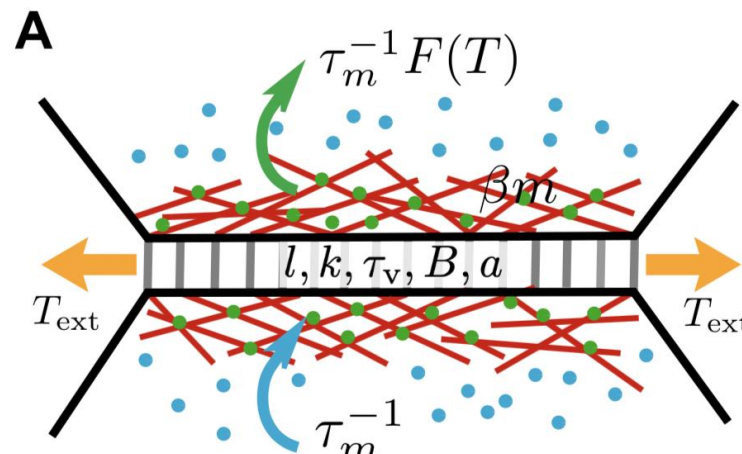
Statistically oriented T1s



Emergent flow from oriented active T1s



Active Junction model



Myosin binds and unbinds to cortex, where unbinding rate decreases with tension: **catch-bond mechanism**

$$\tau_m \dot{m} = 1 - mF(T), \quad F'(T) < 0$$

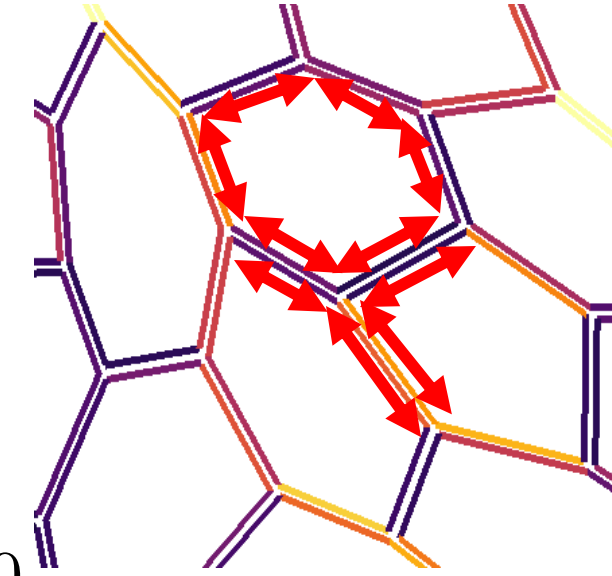
$$F(T) = 1 + e^{-k_0(T-T^*)}$$

- Junctions are viscoelastic springs
- Actomyosin along junctions generates contractility

$$\zeta \dot{l} = -T + T_{\text{ext}}, \quad T = k(l - l_0) + B(l - a) + \boxed{\beta(m - m_0)}$$

$$\tau_v \dot{l}_0 = l - l_0$$

- Feedback loop:** tension increases myosin which increases tension
- Not formally odd, but also an **internal active engine**



Biologically relevant regime:

$$\tau_m, \tau_v \gg \tau_{\text{el}}$$

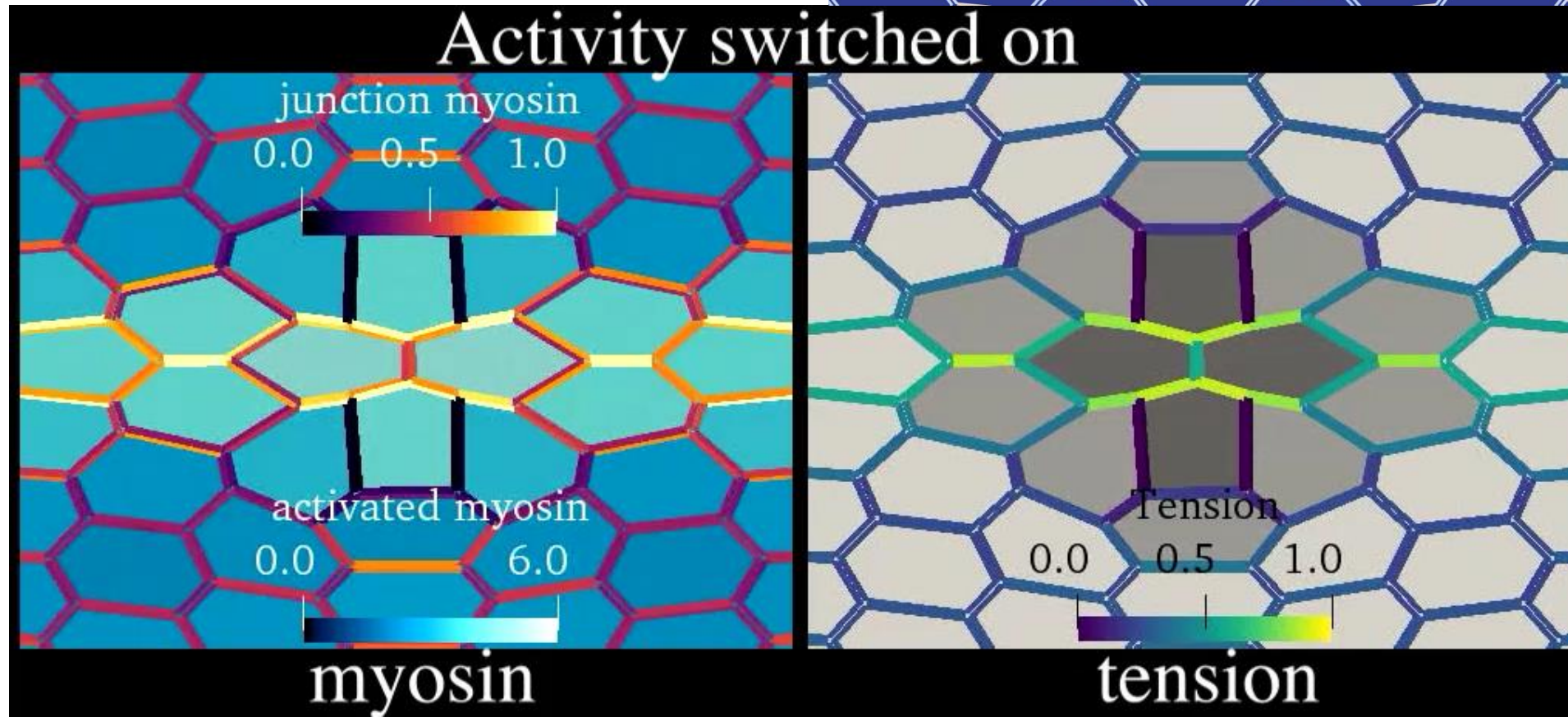
$$\tau_{\text{el}} = \zeta/k \quad \text{elastic time scale}$$

τ_v viscous time scale

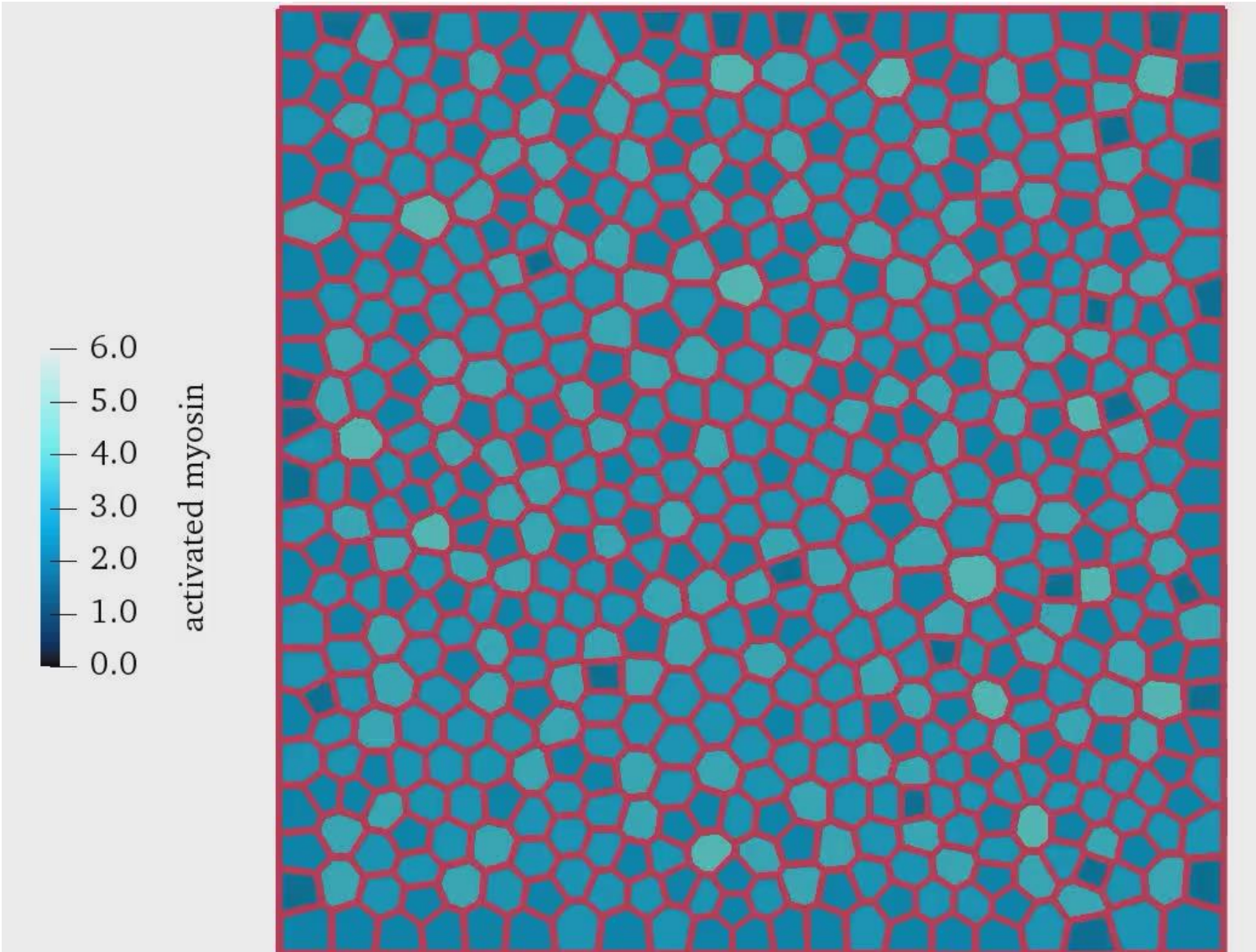
τ_m myosin time scale

Single active T1 transition

R Sknepnek, I Djafer-Cherif, CJ Weijer
and SH, Elife 12, e79862 (2023)



Collective dynamics: Convergence-extension flow & tension chains

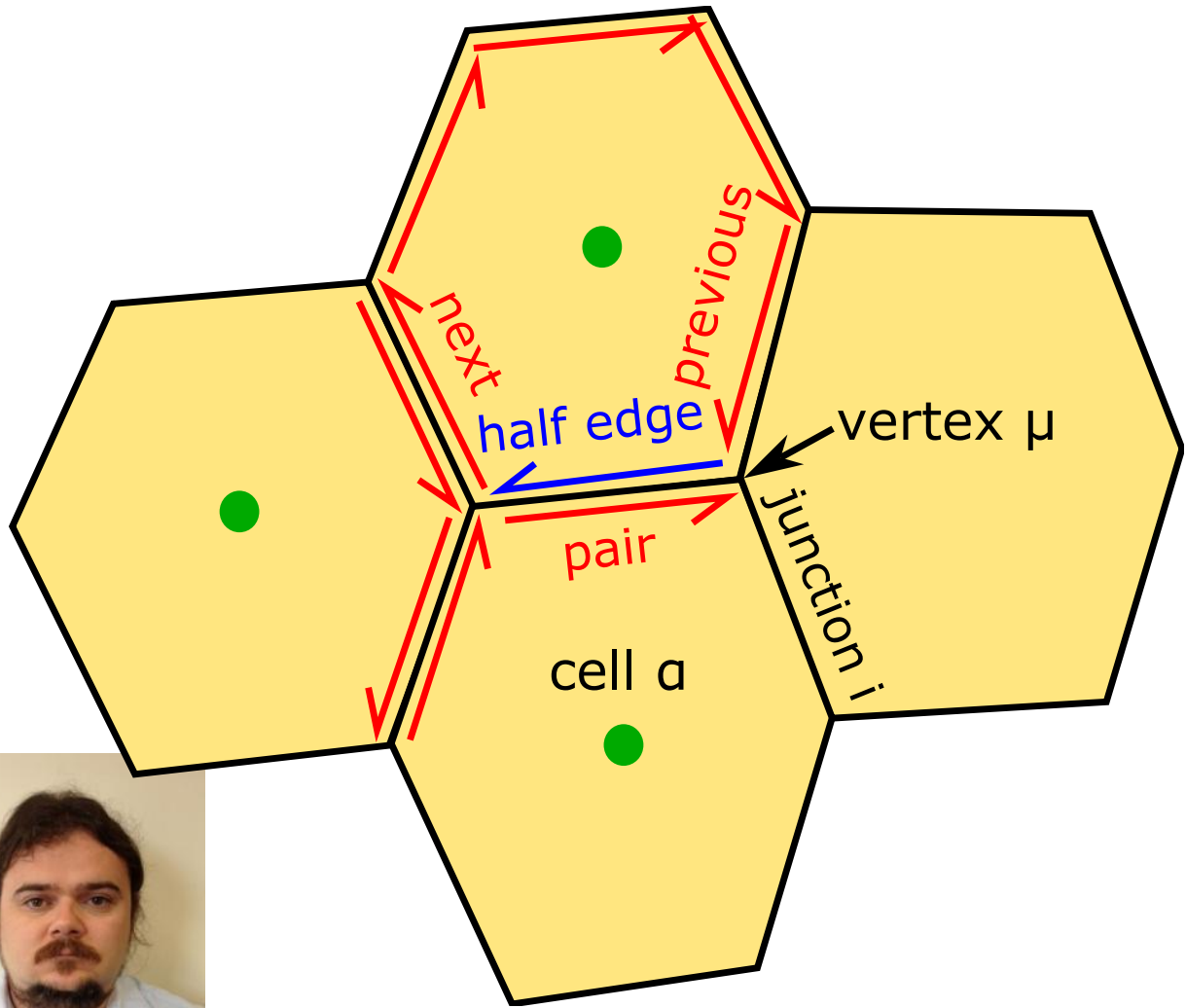


R Sknepnek, I Djafer-Cherif, CJ Weijer and SH, Elife 12, e79862 (2023)

Equivalent to a negative shear modulus / negative viscosity that performs work.

Full continuum analysis:
Ioratim-Uba, Liverpool, SH, PRL 2023

Simulations on a mesh



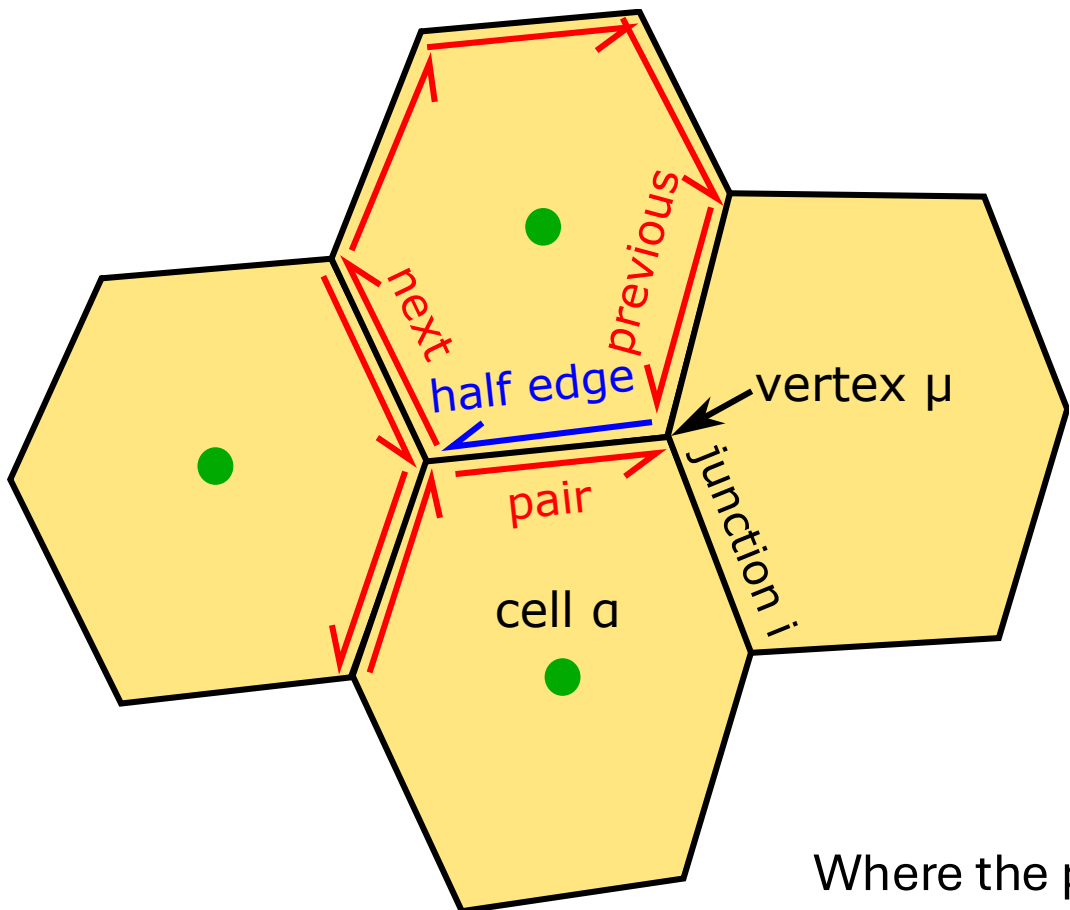
To construct an effective vertex model simulation, we use a half edge data structure:

- Assign every junction a half edge and a paired one, one for each of the cells involved.
- Go around a cell to calculate area A and perimeter P using `half_edge->next` and iterate until returning to the first half edge.
- Go around one vertex by using `half_edge->next` and then `half_edge->pair` and iterate until returning to the original half edge.

Construct specialised ‘Mesh’ class in C++ or python

Method also used for surface triangulations in membrane simulations

Example: Internal activity in a standard vertex model



Overdamped equation of motion for vertex μ :

$$\zeta \dot{\mathbf{r}}_\mu = \sum_i T_i \hat{\mathbf{l}}_i + \sum_\alpha \mathbf{F}_\alpha$$

Tension along the junction:

$$T_i = \Gamma(P_{i,\alpha} - P_0) + \Gamma(P_{i,\beta} - P_0) + T_i^{\text{act}}$$

Area forces orthogonal to the junctions:

$$\mathbf{F}_\alpha = [-\kappa(A_\alpha - A_0) + F_\alpha^{\text{act}}](\mathbf{l}_1 + \mathbf{l}_2) \times \hat{\mathbf{z}}$$

Where the passive forces derive from the Vertex model potential:

$$V = \sum_\alpha \frac{\kappa}{2}(A_\alpha - A_0)^2 + \frac{\Gamma}{2}(P_\alpha - P_0)^2$$

Concrete case: Ornstein-Uhlenbeck junctions

$$\tau \dot{T}_i^{act} = -T_i^{act} + \sqrt{2\sigma^2\tau}\eta_i$$

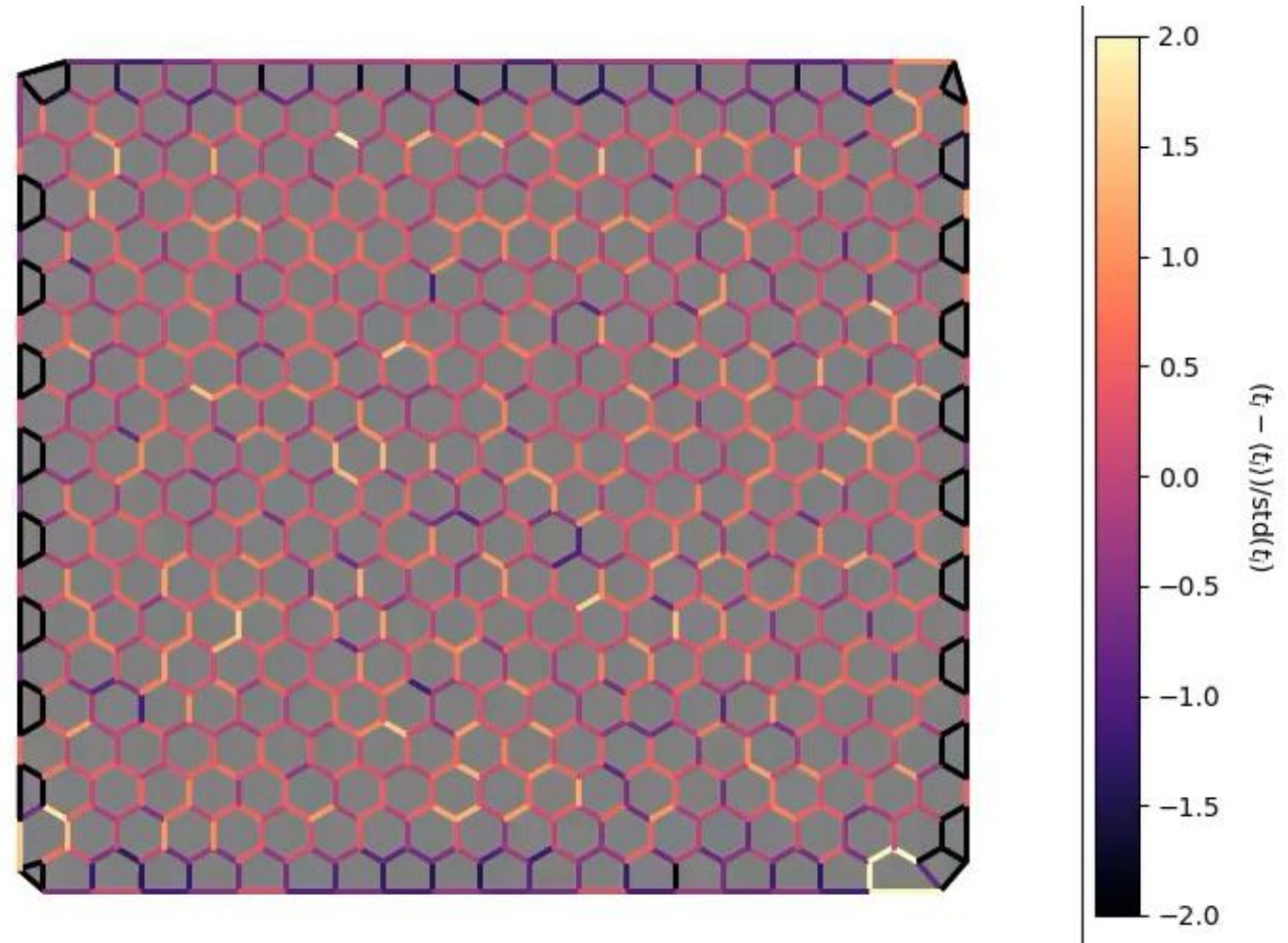
τ persistence time

σ^2 variance (active strength)

$$\langle \eta_i(t)\eta_j(t') \rangle = \delta_{ij}\delta(t-t')$$



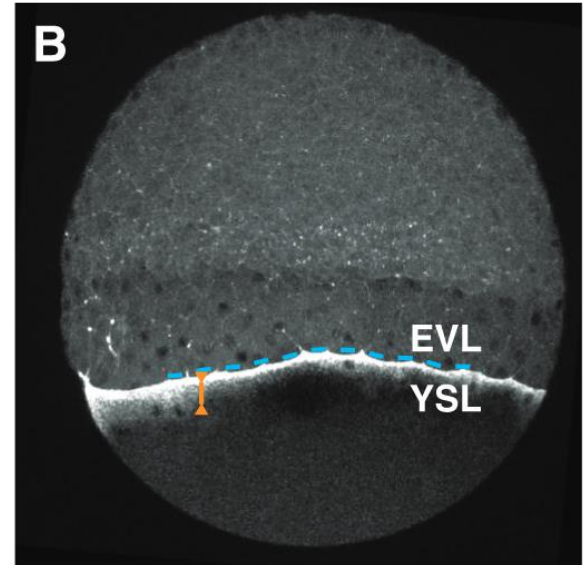
Yann-Edwin Keta



Outlook: The future

- Going to the 3rd dimension in a computationally good way
- Including coupled reaction-diffusion equations
- Division, multiple cell types
- Quantitative link to Biology using model systems like organoids

Zebrafish epiboly
M. Behrnd et al,
Science 2012



Intestinal organoid
(image: Zeiss)

